

1	<u>On-line Methods and Supplementary information</u>	
2	1. Sequence and assembly.....	3
3	1.1 From Duroc 2-14 DNA to Sscrofa11.1 assembly	3
4	1.1.1 Sample, sequencing and assembly	3
5	1.1.2 Contig quality assessment and contig splitting	3
6	1.1.3 Scaffolding	4
7	1.1.4 Gap filling	4
8	1.1.5 Targeted BAC sequencing to fill gaps	5
9	1.1.6 Polishing	6
10	1.2 From MARC1423004 DNA to assembly USMARCv1.0.....	6
11	1.2.1 Sample, sequencing and assembly	6
12	1.2.3 Scaffolding	8
13	1.1.4 Gap filling	8
14	1.2.5 Polishing	8
15	1.3 Anchoring the assemblies to chromosomes	9
16	1.3.1 Chromosome Preparation.....	9
17	1.3.2 Preparation and Selection of BAC clones for FISH.....	9
18	1.3.3 Fluorescence <i>in situ</i> hybridisation.....	9
19	1.4 Quality Assessment of Sscrofa11.1 and USMARCv1.0 assemblies.....	15
20	1.4.1 Order and orientation	15
21	1.4.2 BUSCO and Cogent analyses	19
22	1.4.3 Assemblytics	20
23	2. Analyses.....	26
24	2.1 Repeat analysis.....	26
25	2.1.1 Telomeres.....	28
26	2.1.2 Centromeres	29
27	2.2 Transcriptome data used for building gene models	31
28	2.2.1 Iso-Seq	31
29	2.2.2 RNA-Seq.....	33
30	2.3 SNP chip variants.....	35
31	2.3.1 SNP chip probes mapped to assemblies.....	35
32	3. Annotation (Ensembl).....	38
33	3.1 Repeat Finding	38
34	3.2 Raw computes.....	38
35	3.3 Generation of gene models	39

36	3.3.1 cDNA alignments.....	39
37	3.3.2 PacBio Iso-Seq transcript data	39
38	3.3.3 Protein-to-genome alignment.....	40
39	3.3.4 RNA-seq pipeline.....	41
40	3.3.5 IG and TR genes	43
41	3.3.6 Olfactory receptor genes	43
42	3.3.7 Selenocysteine proteins.....	43
43	3.3.8 Filtering the models	43
44	3.3.9 Collapsing the transcript set.....	43
45	3.3.10 Addition of UTR to coding models.....	46
46	3.3.11 Generating multi-transcript genes	46
47	3.3.12 Pseudogenes.....	46
48	3.3.13 Small ncRNAs	46
49	3.3.14 lincRNAs discovery	46
50	3.3.15 Cross-referencing and stable identifiers.....	47
51	3.3.16 Gene expression	47
52	3.3.17 Comparison of Ensembl and NCBI annotation.....	47
53	3.3.18 Annotation of the USMARCv1.0 assembly.....	48
54	4. References.....	49
55	5. Further supplementary figures	54
56		
57		

58 1. Sequence and assembly

59 1.1 From Duroc 2-14 DNA to Sscrofa11.1 assembly

60 1.1.1 Sample, sequencing and assembly

61 DNA was extracted from Duroc 2-14 cultured fibroblast cells passage 16-18 using the
62 Qiagen Blood & Cell Culture DNA Maxi Kit, producing 139.15 µg DNA from three
63 extractions. The high molecular weight DNA from this extraction was sequenced by Pacific
64 Biosciences (PacBio) using their long read sequencing technology. Libraries for SMRT
65 sequencing were prepared and sequenced as described previously (Pendleton *et al.*, 2015)
66 using P6-C4 chemistry on the RSII using 213 SMRT cells. Initial read statistics are detailed
67 in supplementary table ST1.

68 **Supplementary Table ST1:** Pacific Biosciences read statistics

	TJTabasco (Duroc 2-14)	MARC1423004
Chemistry	P6/C4	P5/C3 and P6/C4
Number of reads	12,328,735	32,960,338
Total length of reads (bp)	175,934,815,397	186,973,885,772
Mean read length (bp)	14,270	6,144
Read N50 (bp)	19,786	9,277

69
70 Contigs were assembled using the Falcon v0.4.0 assembly pipeline following the standard
71 protocol. Quiver v. 2.3.0 (Chin *et al.*, 2013) was used to correct the primary and alternative
72 contigs. Only the primary pseudo-haplotype contigs were used in the assembly.

73 1.1.2 Contig quality assessment and contig splitting

74 Paired-end Illumina reads from the same individual
75 (<http://www.ebi.ac.uk/ena/data/view/PRJEB9115>) were mapped to the 3,206 haploid contigs
76 and assessed for structural abnormalities using the methods described previously (Warr *et al.*,
77 2015). Briefly, 1,000 bp windows across the contigs were assessed for levels of
78 abnormal mapping including high GC-normalized coverage, improper pairing and

79 unexpected insert sizes. Additionally BAC end sequences (BES) (CHORI-242 library)
80 (Humphray *et al.*, 2007) and fosmids (WTSI_1005 library:
81 <https://www.ncbi.nlm.nih.gov/clone/library/genomic/234/>) (ENA accession:HE000001 –
82 HE565349) (Skinner *et al.*, 2016) from the same individual (i.e. Duroc 2-14) were mapped to
83 the contigs and regions with multiple occurrences of incorrect orientation were examined
84 manually in the Integrative Genomics Viewer (IGV) (Robinson *et al.*, 2011). For 28 contigs
85 where there was consistent evidence of structural disagreement between the contigs and the
86 Illumina reads, BAC ends and fosmids, the contigs were split or trimmed.

87 **1.1.3 Scaffolding**

88 In order to establish an initial scaffold the contigs were mapped to Sscrofa10.2 using
89 Nucmer (v3.23) (Kurtz *et al.*, 2004). The positioning of the contigs was determined by using
90 the longest ascending subset of mapping locations using the show-coords tool from
91 Mummer with the –g flag. Contigs with a %IDY below 95% were excluded. Contigs that
92 mapped to regions substantially larger (>180%) or smaller (<10%) than the contig size were
93 excluded. These tolerances were intentionally lenient due to the inflated gap sizes in the
94 Sscrofa10.2 assembly (e.g. including 50 kb between scaffolds as required by the NCBI
95 submission system in 2011) and highly fragmented nature of certain regions of Sscrofa10.2.
96 Adjacent contigs were merged into a single fasta entry with Ns representing gaps between
97 them. Gaps were estimated from the distance between the mapping locations against
98 Sscrofa10.2, with an upper limit of 50 kb. Several of the remaining contigs were placed by
99 identifying their longest alignment position, if this alignment was more than 50% the length of
100 the contig and overlapped with a gap with a IDY>90% they were placed in the gaps with
101 25 bp gaps either side. 346 contigs covering 2.3 Gb were included in the initial chromosomal
102 scaffolds.

103 **1.1.4 Gap filling**

104 PBJelly (English *et al.*, 2012) was used with the 65X raw PacBio reads to fill the gaps in the
105 scaffolds. Default parameters were used for all stages except the assembly stage where
106 max wiggle (-w) was set to 100 kb and max trim (-t) was set to 1,000 bp. These parameters

107 were changed to account for the extremely inaccurate gap sizes and missing sequence in
108 Sscrofa10.2 that will have influenced the estimated gap sizes, to allow heavily overlapping
109 contigs to be closed and to allow potentially low-quality sequence at the end of contigs to be
110 excluded. Following initial gap filling, PBJelly was rerun on the fasta output from the first
111 round, with the unused contigs from the Falcon output added to the fasta to allow extension
112 of the scaffolds. These contigs had been excluded initially to reduce secondary mapping
113 positions. PBJelly is able to add contigs to the end of scaffolds, but not place whole contigs
114 in gaps, so the initial mapping of contigs to scaffolds was examined to find if any of the
115 contigs that had been excluded in this stage due to overlap with existing contigs might fill the
116 gaps. Contigs were placed on a case-by-case basis if there was evidence of overlap with
117 placed sequence on both sides of the gap, if the initial contig quality control was good, and if
118 placement was well supported by BAC end mapping. Additionally, BACs for which the end
119 sequences mapped to adjacent contigs providing evidence for scaffolding these adjacent
120 contigs and for which finished quality sequence was publically available, were aligned and
121 the gap filled and placed following the same restrictions as the unplaced contigs. On
122 completion of these gap-filling procedures 108 gaps remained. Estimation of the size of the
123 remaining gaps was based on BAC end mapping, using the known median insert size of the
124 CHORI-242 library (see <https://bacpacresources.org>). Any gaps estimated to be <100 bp
125 were sized at 100 bp and unspanned gaps were sized at 50 kb.

126 **1.1.5 Targeted BAC sequencing to fill gaps**

127 Five BACs from the CHORI-242 library were selected for further sequencing (CH242-188M9
128 (SSC16); CH242-323K10 (SSC18); CH242-284F8 (SSC18); CH242-61K12 (SSC1); CH242-
129 168C15 (SSC12)) based on BAC ends mapping either side of gaps. The BAC clones were
130 obtained from BACPAC (<https://bacpacresources.org>) and DNA was extracted using the
131 Epicentre BACMAX DNA purification kit following manufacturer's instructions. The BAC DNA
132 was sequenced using Oxford Nanopore Technologies' MinION sequencer using a barcoded
133 2D library following the discontinued protocol SQK-LSK208 on an R9 flow cell using
134 MinKNOW v1.0.5. Sequences were assembled using Canu (Koren *et al.*, 2017) with default

135 settings and each produced a single contig. The BAC vector sequences were removed from
136 the contigs, the contigs were mapped to the assembly initially with Nucmer to confirm they
137 mapped to the expected locations, with exact positions for placement determined by
138 BWA-MEM (Li, 2013). All five contigs mapped to the expected positions and were placed to
139 close the targeted gaps, leaving 103 gaps in the final Sscrofa11 assembly and closing
140 chromosomes 16 and 18.

141 **1.1.6 Polishing**

142 Error correction was done using Arrow from the GenomicConsensus suite
143 (<https://github.com/PacificBiosciences/GenomicConsensus>) using the original 65X PacBio
144 coverage. This was followed by Pilon (Walker *et al.*, 2014) with fixlist restricted to “bases”,
145 but otherwise using default parameters and paired-end Illumina short read data that provided
146 50x genome coverage.

147 **1.2 From MARC1423004 DNA to assembly USMARCv1.0**

148 **1.2.1 Sample, sequencing and assembly**

149 DNA was isolated from barrow MARC1423004 using a salt extraction method. Briefly, frozen
150 lung tissue was crushed into powder, scraped into a 15 mL tube, and suspended in 4 mL
151 digestion buffer (10 mM NH₄Cl, 400 mM NaCl, 50 mM Na₂EDTA, pH 8.0). Digestion was
152 initiated with 100 µL 20% SDS and 70 µL trypsin (5 mg/ml). This initial digestion was allowed
153 to proceed at room temperature (approximately 22°C) for one hour, and then 200 µL of
154 20% SDS and 50 µL of Proteinase K (50 mg/mL) were added. The digestion was incubated
155 at 55°C in a shaking water bath overnight (16 hours). Another 100 µL of Proteinase K were
156 added and incubation extended for another 1.5 hours, until no remaining tissue pieces could
157 be observed in the solution, and then 10 µL of RNase (10 U/µL) were added followed by
158 additional incubation for one hour. 1.25 mL 5M NaCl was added, mixed by inversion, and
159 the tube was centrifuged at 3200 x g at 4°C. The supernatant was transferred to a fresh
160 15 mL tube, and DNA precipitated by addition of 2.5 volumes of 95% ethanol. The
161 precipitate was removed using a hooked Pasteur pipet, dipped twice in separate tubes of
162 70% ethanol on ice, and allowed to briefly dry in air on the hook. The DNA was then eluted

163 from the hook by placing it under 250 μ L TE buffer (10 mM Tris-HCl, 0.1 mM EDTA) until the
164 pellet slipped off into the buffer. The hook was then removed, and the DNA was allowed to
165 dissolve into the buffer for several days at 4°C until it appeared to be completely dissolved.
166 The high molecular weight DNA from this extraction was sequenced by Pacific Biosciences
167 (PacBio) using their long read sequencing technology. Libraries for SMRT sequencing were
168 prepared and sequenced as described previously (Pendleton *et al.*, 2015) using P5/C3 and
169 P6-C4 chemistry on the RSII. A total of 199 P5/C3 cells and 127 P6/C4 cells were
170 produced. Initial read statistics are detailed in supplementary table ST1. Contigs were
171 assembled using Celera Assembler v8.3rc2 (Berlin *et al.*, 2015) using the command:

```
172  
173     wgs-8.3/Linux-amd64/bin/PBcR -s pacbio.spec -fastq  
174     filtered_subreads.fastq genomeSize=3000000000 -sensitive -l swine  
175     sgeName=swine "sge=-p -500 -A swinenewsens" useGrid=1 scriptOnGrid=1  
176  
177     and spec file:  
178     merSize = 16  
179  
180     ovlMemory = 32  
181     ovlStoreMemory = 32000  
182     ovlThreads = 32  
183     threads = 32  
184     ovlConcurrency = 1  
185     cnsConcurrency = 8  
186     merylThreads = 32  
187     merylMemory = 32000  
188     frgCorrThreads = 16  
189     frgCorrBatchSize = 100000  
190     ovlCorrBatchSize = 100000  
191  
192     useGrid=1  
193     scriptOnGrid=1  
194     ovlCorrOnGrid=1  
195     frgCorrOnGrid=1  
196  
197     sge = -A assembly  
198     sgeScript = -pe threads 1  
199     sgeConsensus = -pe threads 8  
200     sgeOverlap = -pe threads 4 -l mem=2GB  
201     gridEngineMhap = -pe threads 15 -l mem=2GB  
202     sgeCorrection = -pe threads 15 -l mem=2GB  
203     sgeOverlapCorrection = -pe threads 1 -l mem=16GB  
204     sgeFragmentCorrection=-pe threads 2 -l mem=2GB  
205     sgeOverlapCorrection=-pe threads 1 -l mem=4GB  
206  
207     asmOvlErrorRate=0.1  
208     asmUtgErrorRate=0.06  
209     asmCgwErrorRate=0.1  
210     asmCnsErrorRate=0.1  
211     asmOBT=1  
212     asmObtErrorRate=0.08
```

```
213     asmObtErrorLimit=4.5
214
215     batOptions=-RS -NS -CS
216     utgGraphErrorRate=0.055
217     utgGraphErrorLimit=4
218     utgMergeErrorRate=0.055
219     utgGraphErrorLimit=4
220
221     ovlHashBits=24
222     ovlHashLoad=0.80
223
224     ovlHashBlockLength      =300000000
225     ovlRefBlockLength      =0
226     ovlRefBlockSize        =2000000
227
```

228 This initial assembly was 2.67 Gbp in 16,441 contigs and an N50 of 2.8 Mbp. Quiver from
229 SMRTportal v. 2.3.0 (Chin *et al.*, 2013) was used to correct the assembly.

230 **1.2.3 Scaffolding**

231 The lung tissue from the pig was sent to Dovetail Genomics (Santa Cruz) for scaffolding by
232 Chicago and HiRise as described (Putnam *et al.*, 2016). This process identified 270 putative
233 misjoins in the contigs and output scaffolds 13,039 scaffolds (294 > 50 kb). The total length
234 was 2.66 Gbp and scaffold N50 was 36.5 Mbp. The dovetail scaffolds were gap-filled where
235 a single contig spanned the gap, correcting false breaks made by HiRise. The resulting
236 assembly was used for reference-guided scaffolding based on the Sscrofa11.1 reference. In
237 case of conflicts, with the exception of cross-chromosome joins, the USDA assembly was
238 unchanged.

239 **1.1.4 Gap filling**

240 PBJelly (English *et al.*, 2012) was used with the 65X raw PacBio reads to fill the gaps in the
241 scaffolds. Default parameters were used for all steps.

242 **1.2.5 Polishing**

243 Gap filling was followed by Pilon (Walker *et al.*, 2014) with fixlist restricted to “bases”, but
244 otherwise using default parameters and paired-end Illumina short read data that provided
245 50x genome coverage. The final assembly of 2.8 Gbp has a scaffold N50 of 131.5 Mbp and
246 a contig N50 of 6.4 Mbp (Table 1).

247

248 **1.3 Anchoring the assemblies to chromosomes**

249 **1.3.1 Chromosome Preparation**

250 Heparinized blood samples were cultured for 72 h in PB MAX Karyotyping medium
251 (Invitrogen) at 37°C, 5% CO₂. Cell division was arrested by adding colcemid at a
252 concentration of 10.0 µg/ml (Gibco) for 30 min prior to hypotonic treatment with 75 mM KCl
253 and fixation to glass slides using 3:1 methanol:acetic acid.

254 **1.3.2 Preparation and Selection of BAC clones for FISH**

255 BAC clones with inserts of approximately 150 kb in size were selected for position using the
256 Sscrofa10.2 NCBI database (www.ncbi.nlm.nih.gov) and ordered from the PigE-BAC library
257 (ARK-Genomics) (Anderson *et al.*, 2000) and the CHORI-242 Porcine BAC library
258 (BACPAC, <https://bacpacresources.org/>). BAC clone DNA was isolated using the Qiagen
259 Miniprep Kit (Qiagen) prior to amplification and direct labelling by nick translation. Probes
260 were labelled with Texas Red-12-dUTP (Invitrogen) and FITC- Fluorescein-12-UTP (Roche)
261 prior to purification using the Qiagen Nucleotide Removal Kit (Qiagen).

262 **1.3.3 Fluorescence *in situ* hybridisation**

263 Metaphase preparations were fixed to slides and dehydrated through an ethanol series
264 (2 min each in 2×SSC, 70%, 85% and 100% ethanol at RT). Probes were diluted in a
265 formamide buffer (Cytocell) with Porcine Hybloc (Insight Biotech) and applied to the
266 metaphase preparations on a 37°C hotplate before sealing with rubber cement. Probe and
267 target DNA were simultaneously denatured for 2 mins on a 75°C hotplate prior to
268 hybridisation in a humidified chamber at 37°C for 16 h. Slides were washed post
269 hybridisation in 0.4x SSC at 72°C for 2 mins followed by 2x SSC/0.05% Tween 20 at RT for
270 30 secs, and then counterstained using VECTASHIELD anti-fade medium with DAPI (Vector
271 Labs). Images were captured using an Olympus BX61 epifluorescence microscope with
272 cooled CCD camera and SmartCapture (Digital Scientific UK) system.

273 The Sscrofa11.1 and USMARCv1.0 assemblies were searched using BLAST with
274 sequences derived from the BAC clones which had been used as probes for the FISH
275 analyses. For most BAC clones these sequences were BAC end sequences (Humphray *et*

276 *al.*, 2007), but in some cases these sequences were incomplete or complete BAC clone
277 sequences (Groenen *et al.*, 2012; Skinner *et al.*, 2016). The links between the genome
278 sequence and the BAC clones used in cytogenetic analyses by fluorescent *in situ*
279 hybridization are summarised in Supplementary Table ST2.

280 The fluorescent *in situ* hybridization data indicate that the following chromosomal scaffolds in
281 the USMARCv1.0 are inverted relative to the conventional cytogenetic orientation of the
282 corresponding chromosomes: SSC1, SSC6, SSC7, SSC8, SSC9, SSC10, SSC11, SSC13,
283 SSC14, SSC15, and SSC16. Whilst the USMARCv1.0 assembly of SSC16 appears overall
284 to be in the reverse orientation with respect to the cytogenetic orientation and the
285 Sscrofa11.1 assembly of this chromosome it also appears to harbour sequences at the start
286 of the scaffold that perhaps belong at the other end of the scaffold.

287 The fluorescent *in situ* hybridization results also indicate areas where future assemblies
288 might be improved. For example, the Sscrofa11.1 unplaced scaffolds contig 1206 and
289 contig1914 may contain sequences that could be added to end of the long arms of SSC1
290 and SSC7 respectively. Examples of the primary fluorescent *in situ* hybridisation data are
291 provided in Supplementary Figures SF1a, SF1b.

292

293 **Supplementary Table ST2:** Fluorescent *in situ* hybridisation results using named BAC clones as probes plus sequence matches for
 294 sequences derived from these BAC clones.

Chr	BAC Name	BES	FISH	Scrofa11.1 coordinates	USMARCv1.0 coordinates
1	PigE-232G23	CT070230.1; CT218278.1	1p	1:615,021-619,597	1:280,453,704-280,458,272
1	CH242-248F13	FP340244.3	1p	1:1,470,202-1,660,001	1:279,368,385-279,558,294
1	CH242-151E10	CT239299.1; CT245986.1	1q	unplaced scaffold: Contig1206	1: 6,156,768-6,336,737
2	PigE-117G14	CT074446.1; CT074447.1	2p	2:19,406-161,226	2:537,026-678,808
2	PigE-8G19	CT260033.1; CT260032.1	2p	2:552,031-671,098	2:29,620-146,529
2	CH242-188K23	CU929880	2 cen	2:52,747,463-52,933,130	2:51,728,649-51,908,148
2	CH242-230M23	CT144824.1; CT258059.1	2 cen	2:53,300,582-53,472,497	no match
2	CH242-441A1	CT364255.1; CT364256.1	2 cen	2:53,458,574-53,652,606	2:52,095,251-52,095,932
2	CH242-294F6	CT378635.1; CT378634.1	2q	2:151,178,736-151,402,963	2:145,456,152-145,678,427
3	PigE-168G22	CT094069.1; CT094070.1	3p	3:301,813-509,346	3:218,358-425,025
3	CH242-315N8	CT359002.1; CT359003.1	3q	3:122,720,374-122,869,530	no match
4	PigE-262E12	CT082779.1; CT193441.1	4p	4:37,383-223,717	4: 96,811- 97,511
4	PigE-131J18	CT116562.1; CT171811.1	4p	4:449,934-626,677	4:322,853-499,367
4	PigE-85G21	CT070098.1; CT190031.1	4q	4:130,625,653-130,748,215	4:130,215,908-130,338,404
5	CH242-288F8	CT132004.1; CT211915.1	5p	5:170,319-344,353	5:188,019-362,653
5	PigE-178M22	CT139068.1; CT155898.1	5p	5:175,168-311,462	5:192,886-329,113
5	CH242-133F9	CT166002.1; CT166003.1	5p	5:438,296-633,458	5:456,924-652,458
5	PigE-127K14	CT057696.1; CT057697.1	5p	5:1,003,455-1,129,329	5:1,024,261-1,148,699
5	PigE-74P10	CT188857.1; CT188858.1	5p	5:3,739,938-3,883,755	5:103,338,585-103,481,984
5	PigE-99L23	CT079916.1; CT106700.1	5p Mid	5:31,980,969-32,114,628	no match
5	CH242-63B20	FP102738	5q	5:104,304,289-104,489,770	no match
6	PigE-238J17	CT220438.1; CT220439.1	6p	6:2,333,972-2,522,065	6:162,952,836-163,141,204
6	PigE-199E24	CT272854.1; CT272853.1	6 below cen	6:62,771,286-62,952,647	6:104,969,580-105,152,317
6	CH242-510F2	CT396711.1; CT442620.1	6q	6:170,248,061-170,454,571	6:162,654-369,119
7	PigE-52L22	CT054562.1; CT063652.1	7p	7:188,339-317,255	7:125,463,765-125,463,765
7	PigE-246A1	CT203984.1; CT070741.1	7 cen	7:24,628,314-24,671,828	no match
7	PigE-230H8	CT120917.1	7q below cen	7:46,704,415-46,704,995	7:395,704-396,284
7	PigE-75E21	CT188956.1; CT261917.1	7q below cen	7:46,901,592-47,032,091	7:68,406-199,212
7	CH242-103I13	CU695123.2	7q	Unplaced scaffold: Contig1914	7:7,614,911-7,838,927

Chr	BAC Name	BES	FISH	Sscrofa11.1 coordinates	USMARCv1.0 coordinates
8	PigE-134L21	CT126839.1; CT172501.1	8p	8:570,904-705,341	8:280,369,080-280,502,409
8	PigE-2N1	CT229915.1; CT229916.1	8p	8:819,717-958,131	8:137,599,822-137,737,820
8	PigE-118B21	CT048761.1; CT091504.1	8q	8:138,491,413-138,647,394	8:322,914-478,869
9	CH242-65G4	CU695192.2	9p	9:320,582-511,079	9:137,686,630-137,874,917
9	PigE-126O17	CT170583.1; CT057320.1	9p	9:443,462-603,022	9:137,594,779-137,754,110
9	PigE-242D8	CT123266.1; CT123265.1	9 mid	9:67,752,381-67,910,109	9:71,096,887-71,254,731
9	CH242-411M8	CT362997.1; CT468791.1	9q	9:139,180,446-139,338,710	9:168,756-327,007
10	CH242-451I23	CT369304.1; CT459538.1	10p	Unplaced scaffold: Contig2471	10:71,863,534-72,028,842
10	CH242-36D16	CT345373.1; CT186999.1	10q	10:55,422,866-55,600,351	10:15,300,371-15,480,359
10	CH242-517L16	FP325295.2	10q	10:55,609,778-55,800,022	10:15,098,969-15,290,916
11	PigE-199B10	CT272693.1	11p	11:135,233-297,713	11:79,101,520-79,264,254
11	PigE-232N19	CT193346.1	11p	11:290,540-291,222	11:79,108,017-79,108,697
11	PigE-211E21	CT044498.1; CT044499.1	11p	11:1,584,043-1,743,425	11:77,663,220-77,822,434
11	CH242-239O11	CT146353.1; CT286242.1	11q	11:78,888,491-79,057,526	11:827,483-996,382
12	PigE-253K5	CT081057.1; CT204391.1	12p	12:324,614-524,015	12:3,288-206,400
12	PigE-124G15	CT056668.1; CT092177.1	12q	12:60,846,540-60,990,610	12:58,746,918-58,890,342
13	PigE-197C11	CT271598.1; CT271599.1	13p	13:556,804-694,010	13:204,579,401-204,716,338
13	PigE-179J15	CT124924.1; CT124925.1	13q	13:205,856,740-206,006,912	13:3,005,553-3,154,893
14	PigE-137C12	FP340551.3	14p	14:17,423-156,591	14:140,940,126-140,804,938
14	PigE-167E18	CT089616.1; CT089617.1	14q	14:141,407,495-141,435,234	14:98,899-125,652
15	PigE-90C11	CT190903.1; CT190904.1	15p	15:3,442,144-3,596,666	15:139,733,189-139,886,921
15	PigE-108N22	CT073138.1; CT046453.1	15 mid	15:56,903,229-57,028,679	no match
15	CH242-170N3	FP236135.2	15q	15:139,616,279-139,784,756	15:3,511,408-3,588,855
16	PigE-90L22	CT191132.1; CT113297.1	16p	16:109,696-235,547	16:87,402-212,531
16	PigE-124C22	CT056551.1; CT056550.1	16p	16:117,329-308,428	16:94,873-287,243
16	CH242-4G9	CT041970.1; CT041969.1	16p	16:141,557-324,802	16:118,753-303,587
16	PigE-173H6	CT123878.1; CT123877.1	16p	16:167,106-299,570	16:144,276-278,432
16	PigE-149F10	CT088298.1; CT153977.1	16p	16:596,671-782,524	16:78,918,129-79,108,868
16	CH242-42L16	CT347302.1; CT347303.1	16q	16:79,097,179-79,303,695	16:878,687-1,085,418
17	CH242-70L7	CT077340.1; CT077341.1	17p	17:545,995-673,770	17:464,378-592,438
17	PigE-190G24	CT126644.1; CT096362.1	17p	17:515,422-707,787	17:433,829-626,496
17	CH242-243H19	CT321876.1; CT321877.1	17q	17:61,760-582-61,937,945	17:62,450,941-62,628,249

Chr	BAC Name	BES	FISH	Sscrofa11.1 coordinates	USMARCv1.0 coordinates
18	PigE-253N22	CT081116.1; CT204433.1	18p	18:1,616,389-1,751,286	18:1,565,719-1,700,920
18	PigE-202I11	CT042866.1; CT254626.1	18q	18:55,539,630-55,700,409	18:55,320,418-55,481,057
X	CH242-447L20	CT377508.1; CT467360.1	Xp	X:505,086-692,549	no match
X	CH242-156O11	FP074895.7	Xp + Yp	X:6,337,709-6,584,993	X:7,588,110-7,597,109
X	CH242-19N1	CU856094.8	Xp	X:6,705,194-6,834,183	X:7,588,110-7,715,932
X	CH242-305A15	CU861979.13	Xq	X:125,384,028-125,529,813	X:126,150,718-126,296,945
Y	CH242-156O11	FP074895.7	Xp + Yp	Y:4,744,231-4,791,971	Y:32,909,634-32,923,401

295

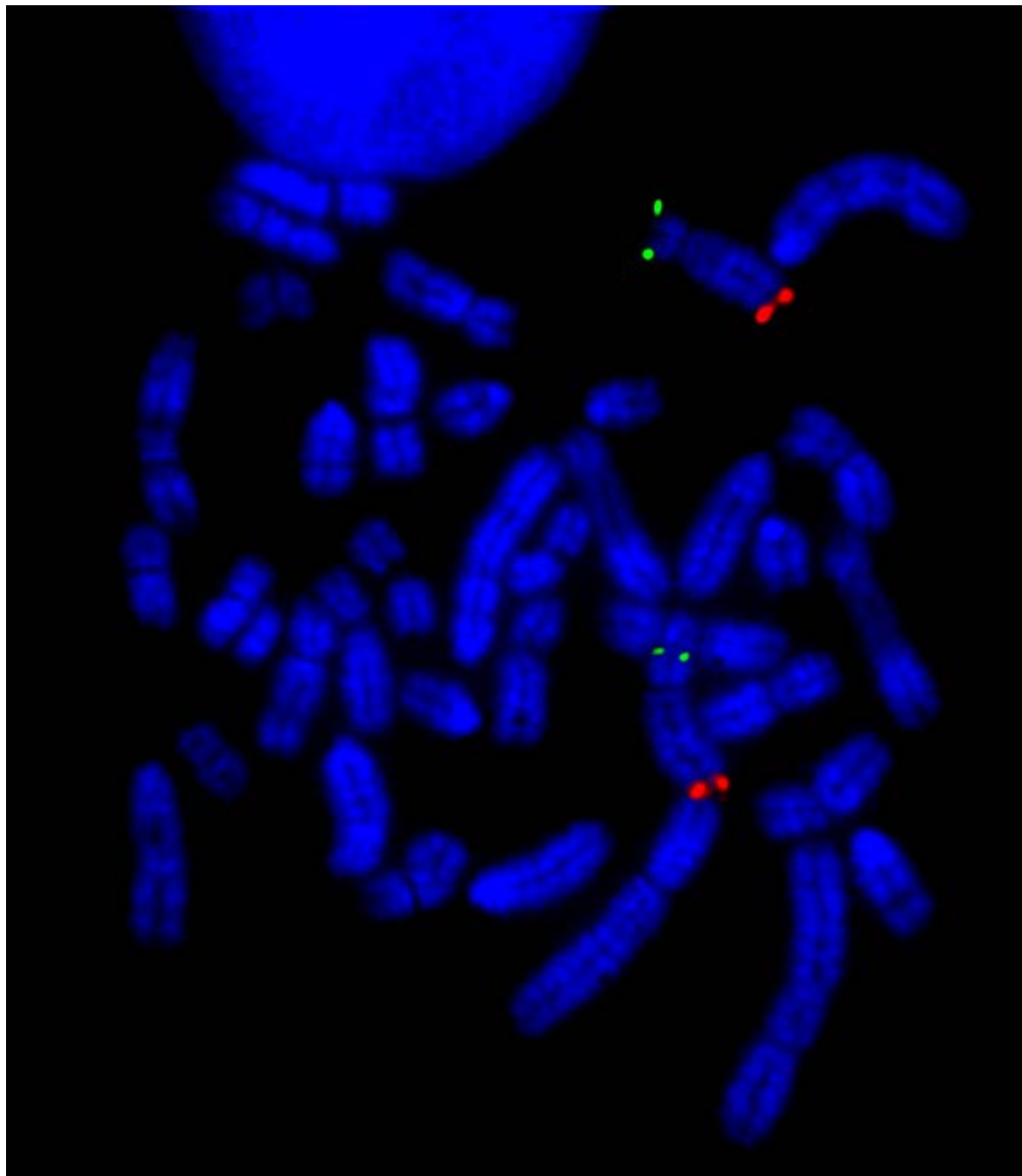
296

297

298 **Supplementary Figure SF1a:** Fluorescent *in situ* hybridisation assignments

299 a. SSC6 – p-telomeric end labelled with PigE-238J17, q-telomeric end labelled with CH242-

300 510F2



301

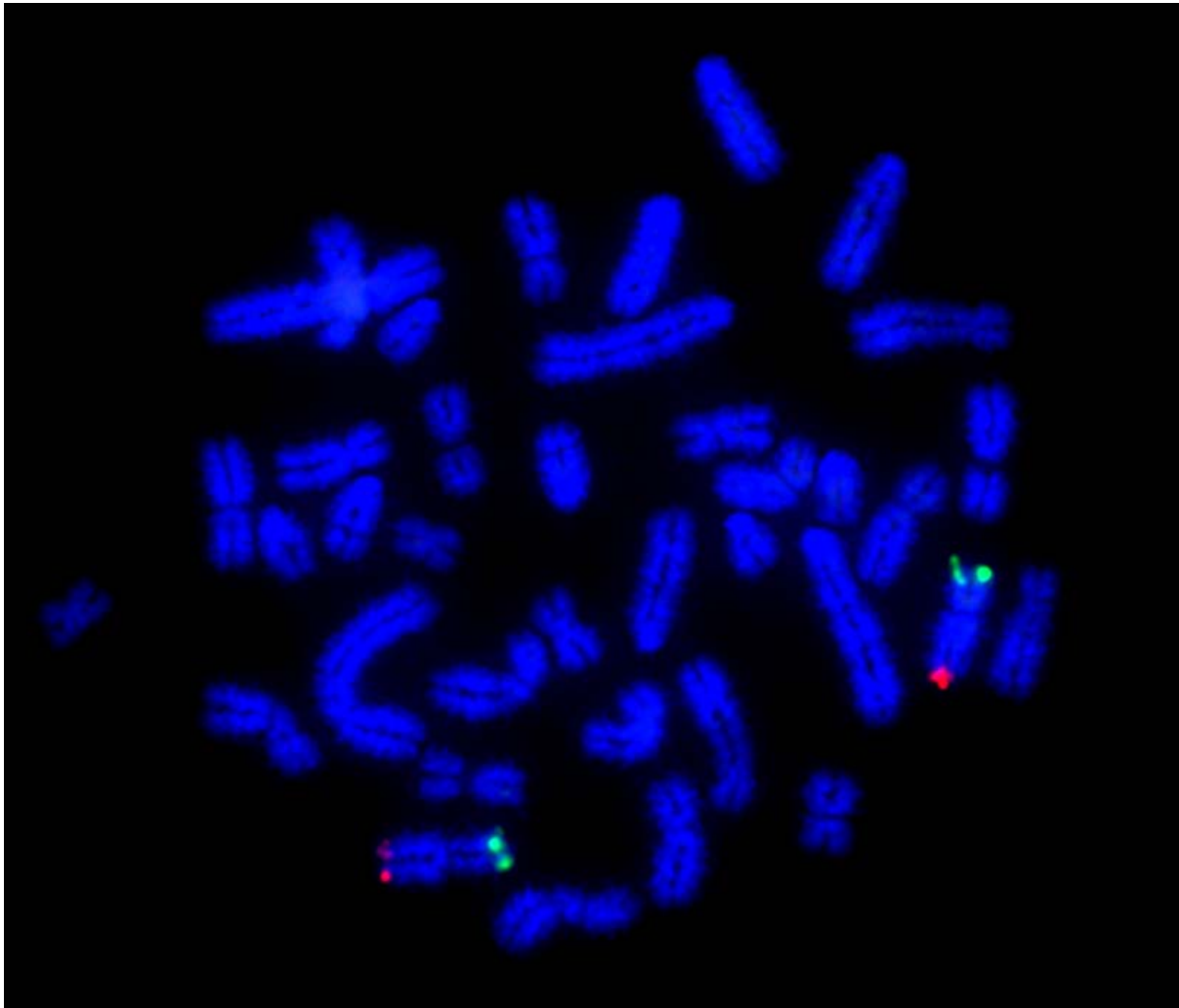
302

303

304

305 **Supplementary Figure SF1b:** Fluorescent *in situ* hybridisation assignments

306 b. SSCX – p-telomeric end labelled with CH242-19N1, q-telomeric end labelled with CH242-
307 305A15



308

309

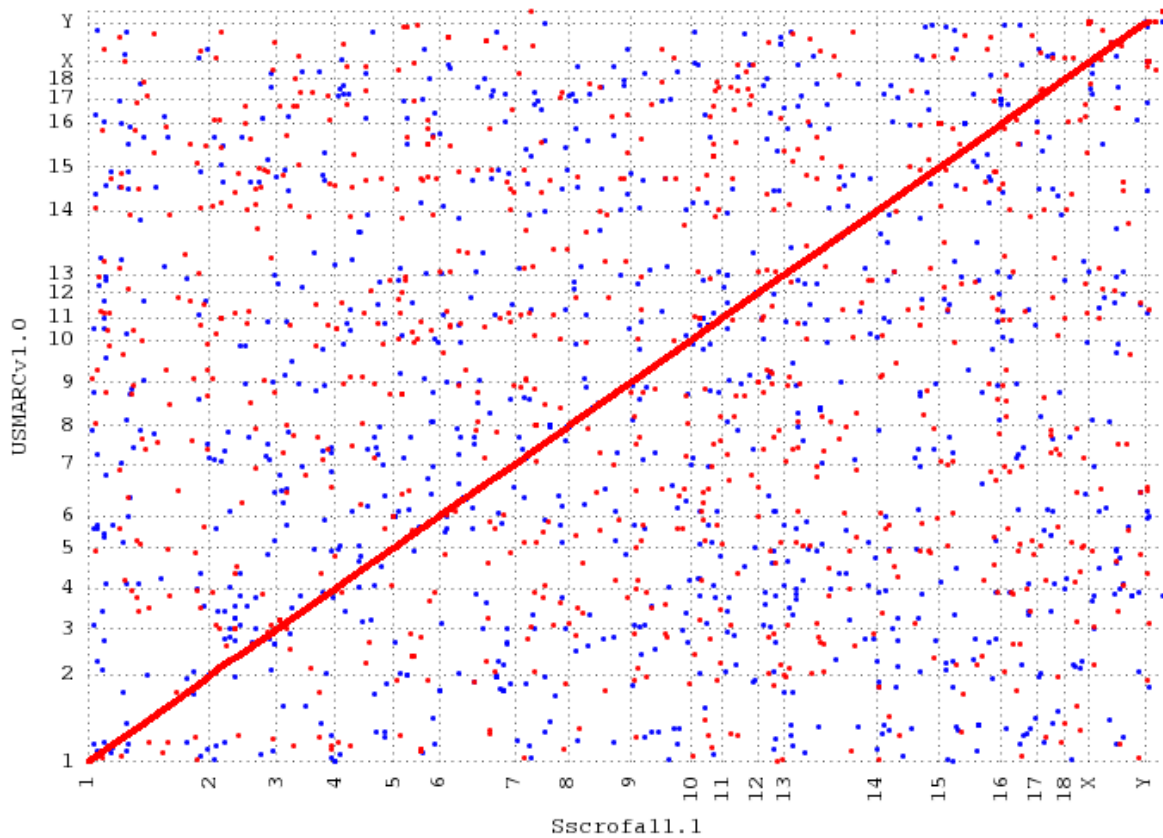
310 **1.4 Quality Assessment of Sscrofa11.1 and USMARCv1.0 assemblies**

311 **1.4.1 Order and orientation**

312 In addition to assigning and orienting the scaffolds on chromosomes as described above,
313 order and orientation within chromosome assemblies was checked by alignment to the
314 radiation hybrid map (Servin *et al.*, 2012) and alignments amongst the assemblies
315 (Sscrofa10.2, Sscrofa11.1 and USMARCv1.0). The overall alignments indicate that the new
316 assemblies (Sscrofa11.1, USMARCv1.0) are essentially co-linear with each other and with
317 the radiation hybrid map (Figure 1, Supplementary Figure SF2). At the level of individual

318 chromosomes, order and orientation within chromosome 18, for example, is consistent
319 between Sscrofa11.1 and USMARCv1.0 and both SSC18 chromosome assemblies are
320 supported by the radiation hybrid map (Supplementary Figure SF3). However, although the
321 alignments of other chromosomes with the radiation map also support the overall co-linearity
322 of the sequence and radiation hybrid maps, there are some differences in local order and
323 orientation between the Sscrofa11.1 and USMARCv1.0 as illustrated in Supplementary
324 Figures SF4 and SF5 for SSC7 and SSC8 respectively.

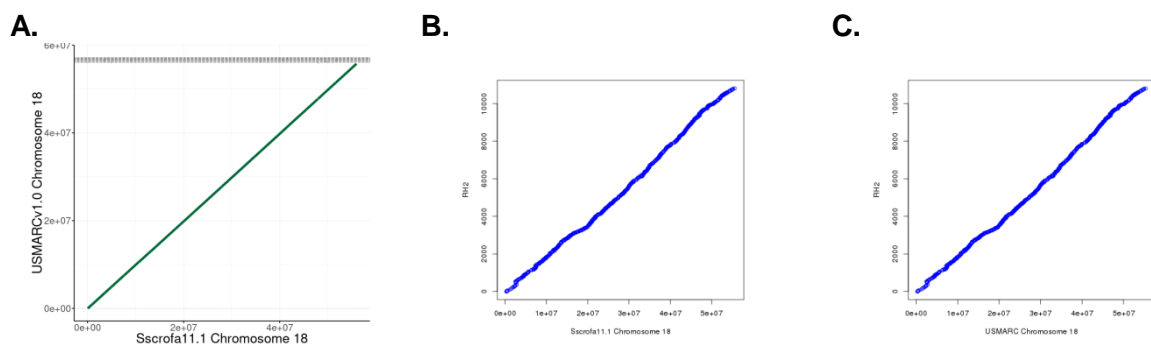
325



326

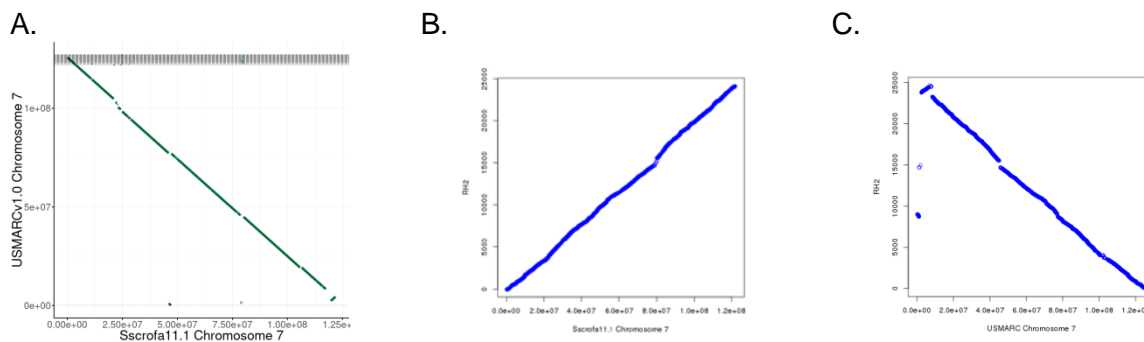
327 **Supplementary Figure SF2:** Alignment of Sscrofa11.1 and USMARCv1.0 assemblies after
 328 correcting inversions of USMARCv1.0 chromosome scaffolds

329

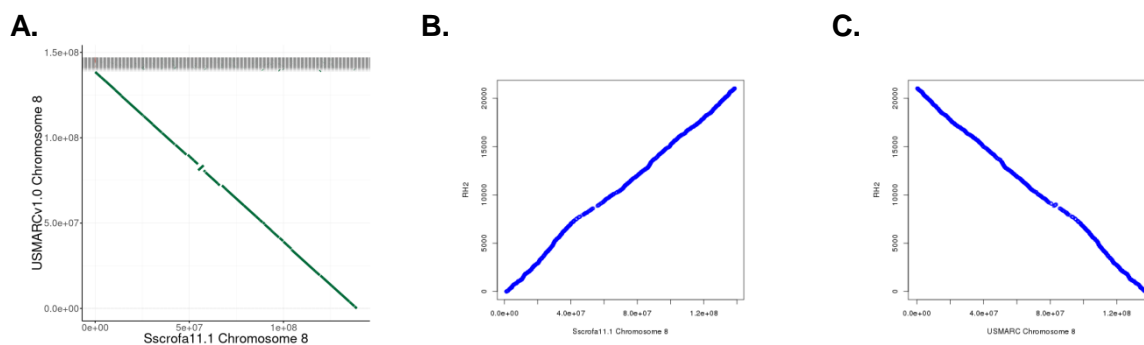


330 **Supplementary Figure SF3:** Order and orientation of SSC18 assemblies: A. alignment of
 331 Sscrofa11.1 and USMARCv1.0 assemblies of SSC18; B. alignment of Sscrofa11.1 and
 332 radiation hybrid map (RH2); C. alignment of USMARCv1.0 and radiation hybrid map (RH2).

333



335 **Supplementary Figure SF4:** Order and orientation of SSC7 assemblies: **A.** alignment of
 336 Sscrofa11.1 and USMARCv1.0 assemblies of SSC7; **B.** alignment of Sscrofa11.1 and
 337 radiation hybrid map (RH2); **C.** alignment of USMARCv1.0 and radiation hybrid map (RH2).



338 **Supplementary Figure SF5:** Order and orientation of SSC8 assemblies: **A.** alignment of
 339 Sscrofa11.1 and USMARCv1.0 assemblies of SSC8; **B.** alignment of Sscrofa11.1 and
 340 radiation hybrid map (RH2); **C.** alignment of USMARCv1.0 and radiation hybrid map (RH2).

341 The matches shown in the grey zone at the top of each plot of the Sscrofa11.1 versus
 342 USMARCv1.0 alignments probably represent a mix of repetitive sequences and matches to
 343 the unplaced scaffolds in the USMARCv1.0 assembly.

344 Whether the differences between Sscrofa11.1 and USMARCv1.0 in order and orientation
 345 within chromosomes represent assembly errors or real chromosomal differences will require
 346 further research. The sequence present at the telomeric end of the long arm of chromosome
 347 7 (after correcting the orientation of the USMARCv1.0 SSC7 assembly) is missing from the
 348 Sscrofa11.1 SSC7 assembly, and currently located on a 3.8 Mbp unplaced scaffold
 349 (AEMK02000452.1) that harbours several genes including DIO3, CKB and NUDT14 whose

350 orthologues map to human chromosome 14 as would be predicted from the pig-human
351 comparative map (Meyers *et al.*, 2005). This omission will be corrected in an updated
352 assembly in future.

353 **1.4.2 BUSCO and Cogent analyses**

354 The assembly was assessed for completeness using BUSCO (Simão *et al.*, 2015) (Table
355 ST3) and Cogent (<https://github.com/Magdoll/Cogent>), and assessed for structural accuracy
356 by checking consistency between markers from radiation hybrid maps (Servin *et al.*, 2012)
357 and the assembly. PacBio transcriptome (Iso-Seq) data consisting of high-quality isoform
358 sequences from 7 tissues (diaphragm, hypothalamus, liver, skeletal muscle (*longissimus*
359 *dorsi*), small intestine, spleen and thymus) from the pig whose DNA was used as the source
360 for the USMARCv1.0 assembly were pooled together for Cogent analysis. Cogent is a tool
361 that identifies gene families and reconstructs the coding genome using full-length, high-
362 quality (HQ) transcriptome data without a reference genome. Cogent partitioned 276,196 HQ
363 isoform sequences into 30,628 gene families, of which had at least 2 distinct transcript
364 isoforms. Cogent then performed reconstruction on the 18,708 partitions. For each partition,
365 Cogent attempts to reconstruct coding 'contigs' that represent the ordered concatenation of
366 transcribed exons as supported by the isoform sequences. The reconstructed contigs were
367 then mapped back to Sscrofa11.1 and contigs that could not be mapped or map to more
368 than one position are individually examined.

369

370

371 **Supplementary Table ST3: BUSCO statistics, BUSCOv2 (OrthoDBv9)**

	Sscrofa10.2	Sscrofa11.1	USMARCv1.0
Complete BUSCOs	80.9%	93.8%	93.1%
Complete and single-copy BUSCOs	80.2%	93.3%	92.6%
Complete and duplicated BUSCOs	0.7%	0.5%	0.5%
Fragmented BUSCOs	8.2%	3.5%	3.5%
Missing BUSCOs	10.9%	2.7%	3.4%
Total BUSCO groups searched	4,104	4,104	4,104

372

373 **1.4.3 Assemblytics**

374 A comparison of pig genome assemblies was undertaken using the Assemblytics tools
375 (Nattestad and Schatz, 2016) (<http://assemblytics.com>). The comparisons are listed in Table
376 ST4.

377

Reference	Sscrofa10.2 (GCF_000003025.5)	
Query	Assembly accession	
Sscrofa11.1	GCA_000003025.6	http://qb.cshl.edu/assemblytics/analysis.php?code=i0H3KuHhWjKO5Tn7nsXg
USMARCv1.0	GCA_002844635.1	http://qb.cshl.edu/assemblytics/analysis.php?code=faROmPzOIMp1q5ldToO8
Reference	Sscrofa11.1	
Query	Assembly accession	
Sscrofa11.1	GCA_000003025.6	N/A
USMARCv1.0	GCA_002844635.1	http://assemblytics.com/analysis.php?code=4rscWrit7paorSvTMI7L
Bamei	GCA_001700235.1	http://assemblytics.com/analysis.php?code=gpCq8VWG4aWrocriCWww
Berkshire	GCA_001700575.1	http://assemblytics.com/analysis.php?code=dvVxU3qkCNUR3rWpm2FI
Hampshire	GCA_001700165.1	http://assemblytics.com/analysis.php?code=V6jWeDYKywLu4Av40Ikh
Jinhua	GCA_001700295.1	http://qb.cshl.edu/assemblytics/analysis.php?code=UxtEbFk065DWQBpYz0sV
Landrace	GCA_001700215.1	http://qb.cshl.edu/assemblytics/analysis.php?code=7V7QGUCXrNAtFcGL6DMT
LargeWhite	GCA_001700135.1	http://qb.cshl.edu/assemblytics/analysis.php?code=UymCHs1NirQkdMFFbM1e
Meishan	GCA_001700195.1	http://qb.cshl.edu/assemblytics/analysis.php?code=toDVmO7nus0BbyMCGKSc
Pietrain	GCA_001700255.1	http://qb.cshl.edu/assemblytics/analysis.php?code=TIIXYB2uQYgWbf5YqNXk
Rongchang	GCA_001700155.1	http://qb.cshl.edu/assemblytics/analysis.php?code=HzggG8kBPJ6uKWWEvZOV
Tibetan	GCA_000472085.2	http://qb.cshl.edu/assemblytics/analysis.php?code=o9WtylF6wTnGsEeAiizn
Wuzhishan	GCA_000325925.2	http://qb.cshl.edu/assemblytics/analysis.php?code=UbH3avfeoW19DjJmVC8C

380

381 **Supplementary Table ST4b:** Assemblytics comparisons

Reference Query	Assembly accession	USMARCv1.10
Scrofa11.1	GCA_000003025.6	http://assemblytics.com/analysis.php?code=4rscWriT7paorSvTMI7L
USMARCv1.0	GCA_002844635.1	N/A
Bamei	GCA_001700235.1	http://assemblytics.com/analysis.php?code=A1doW581DPkQKXlwfbtB
Berkshire	GCA_001700575.1	http://qb.cshl.edu/assemblytics/analysis.php?code=5dCXFbth2110zsguw58t
Hampshire	GCA_001700165.1	http://qb.cshl.edu/assemblytics/analysis.php?code=Xe5ENqAjsxeNcrK7TaRp
Jinhua	GCA_001700295.1	http://qb.cshl.edu/assemblytics/analysis.php?code=nqEihnLJRPsjNswVxV9J
Landrace	GCA_001700215.1	http://qb.cshl.edu/assemblytics/analysis.php?code=tftrkAXiy148TUsb8HIJ
LargeWhite	GCA_001700135.1	http://qb.cshl.edu/assemblytics/analysis.php?code=IZM3EFMBzo9KyytQMSWH
Meishan	GCA_001700195.1	http://qb.cshl.edu/assemblytics/analysis.php?code=K9qeCrVxr9znPtFanHd3
Pietrain	GCA_001700255.1	http://qb.cshl.edu/assemblytics/analysis.php?code=U1n9D7z7DtRvbWjqEdTH
Rongchang	GCA_001700155.1	http://qb.cshl.edu/assemblytics/analysis.php?code=nEk3faE5s8YYckjNuvN7
Tibetan	GCA_000472085.2	http://qb.cshl.edu/assemblytics/analysis.php?code=NqjCZ7wvt6D0vm7Ai4tN
Wuzhishan	GCA_000325925.2	http://qb.cshl.edu/assemblytics/analysis.php?code=mEqp9WaGi9eceSY4Vid6

382

383

384

385

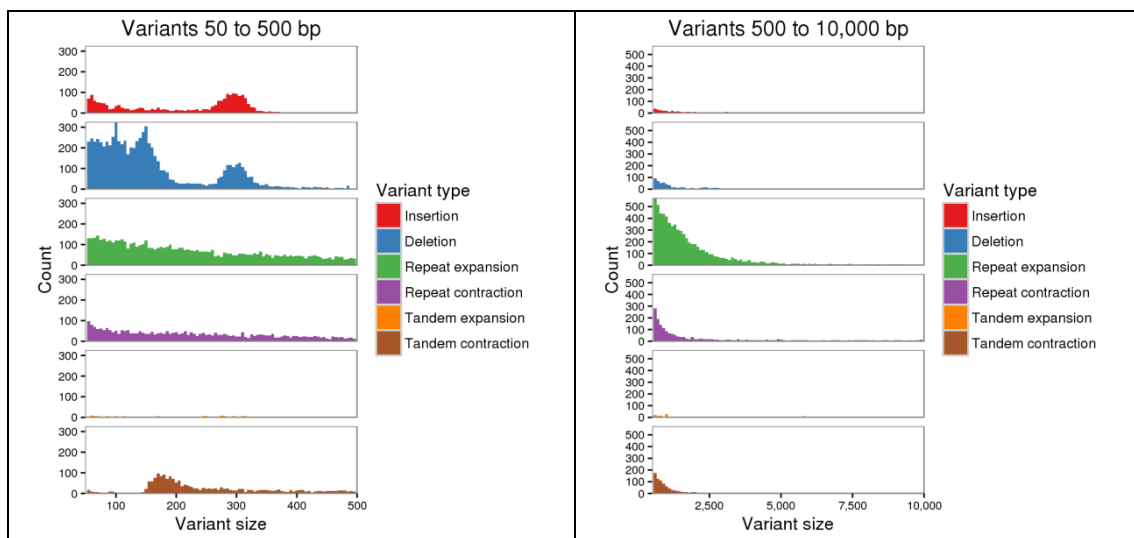
386 **Supplementary Table ST4c:** Assembly statistics* for pig genome assemblies subject to Assemblytics analyses

Assembly	Accession	Total (bp)(ungapped)	Scaffolds	Scaffold N50	Contigs	Contig N50
Sscrofa11.1	GCA_000003025.6	2,472,047,747	706	88,231,837	1,118	48,231,277
USMARCv1.0	GCA_002844635.1	2,623,130,238	14,818	131,458,098	14,818	6,372,407
Bamei	GCA_001700235.1	2,433,636,520	129,335	1,529,027	187,466	70,893
Berkshire	GCA_001700575.1	2,414,739,650	94,468	1,655,397	137,661	94,651
Hampshire	GCA_001700165.1	2,418,011,428	82,206	1,550,023	122,452	102,417
Jinhua	GCA_001700295.1	2,433,032,022	115,554	1,478,908	158,796	95,227
Landrace	GCA_001700215.1	2,420,570,845	94,659	1,407,841	141,909	88,142
LargeWhite	GCA_001700135.1	2,430,896,979	102,342	2,441,555	150,742	88,831
Meishan	GCA_001700195.1	2,438,814,343	133,833	1,248,180	201,146	63,263
Pietrain	GCA_001700255.1	2,415,062,022	88,436	1,663,542	139,497	80,611
Rongchang	GCA_001700155.1	2,429,730,895	120,246	2,325,000	173,508	79,093
Tibetan	GCA_000472085.2	2,379,878,366	72,068	861,885	148,234	57,199
Wuzhishan	GCA_000325925.2	2,453,484,489	137,577	5,853,977	272,163	31,939

387 * source NCBI Assembly

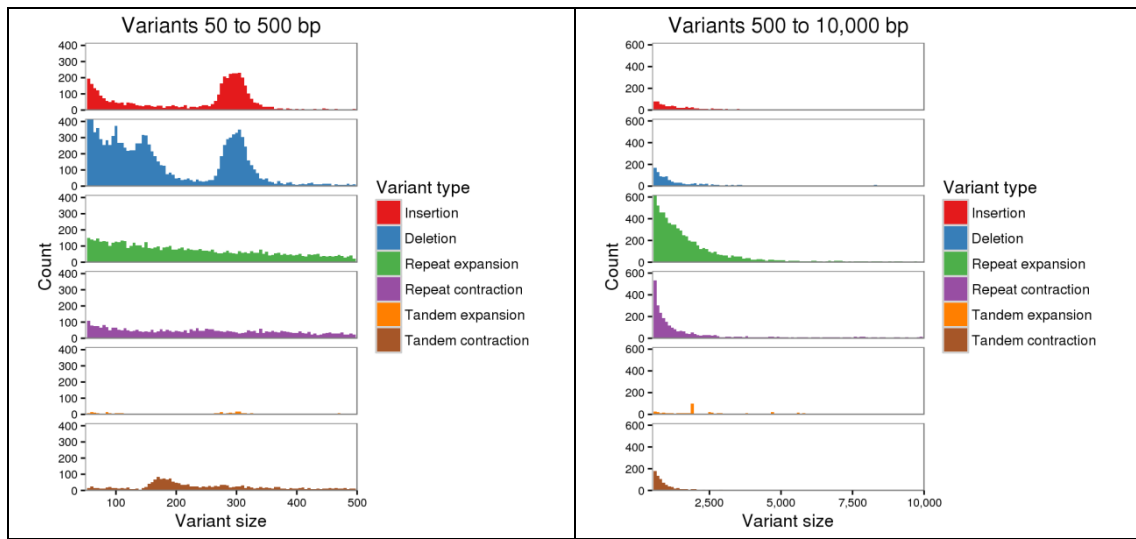
388

389 In all the pairwise comparisons amongst the former Sscrofa10.2 assembly and the new
 390 Sscrofa11.1 an USMARCv1.0 assemblies there is a peak of insertions and deletion with
 391 sizes of about 300 bp (Supplementary Figures SF6a-c). We assume that these correspond
 392 to SINE elements. Despite the fact that the Sscrofa10.2 and Sscrofa11.1 assemblies are
 393 representations of the same pig genome, there are many more differences between these
 394 assemblies than between the Sscrofa11.1 and USMARCv1.0 assemblies. We conclude that
 395 many of the differences between the Sscrofa11.1 assembly and the earlier Sscrofa10.2
 396 assemblies represent improvements in the former. Some of the differences may indicate
 397 local differences in terms of which of the two haploid genomes has been captured in the
 398 assembly. The differences between the Sscrofa11.1 and USMARCv1.0 will represent a mix
 399 of true structural differences and assembly errors that will require further research to resolve.
 400



401
 402 **Supplementary Figure SF6a:** Assemblytics comparison of Sscrofa11.1 (query) against the
 403 Sscrofa10.2 (reference) i). (left hand panel) variants from 50 to 500 bp; ii). (right hand panel)
 404 variants from 500 to 10,000 bp.
 405

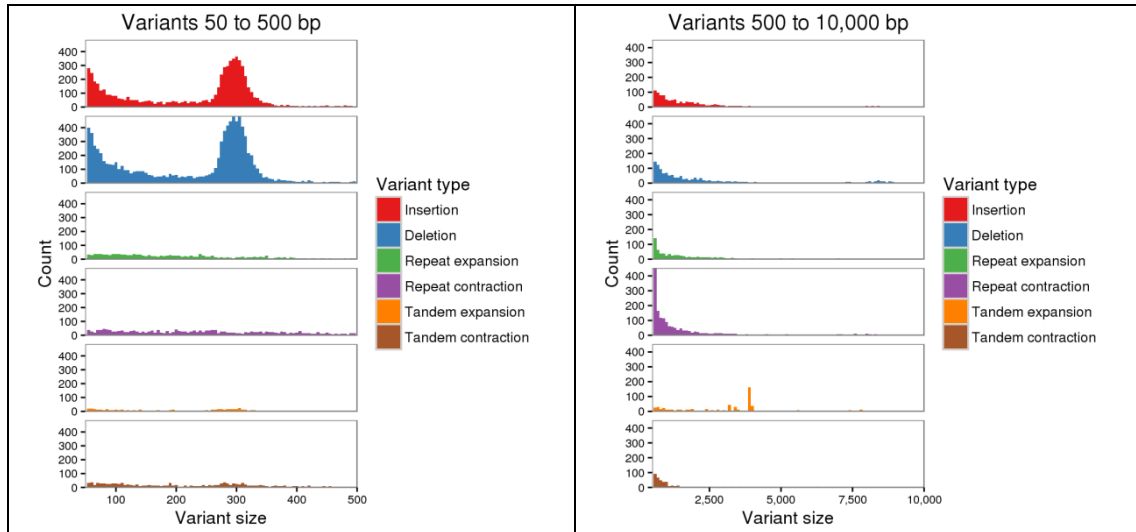
406



407

408 **Supplementary Figure SF6b:** Assemblytics comparison of USMARCv1.0 (query) against
409 the Sscrofa10.2 (reference) i). (left hand panel) variants from 50 to 500 bp; ii). (right hand
410 panel) variants from 500 to 10,000 bp.

411



412

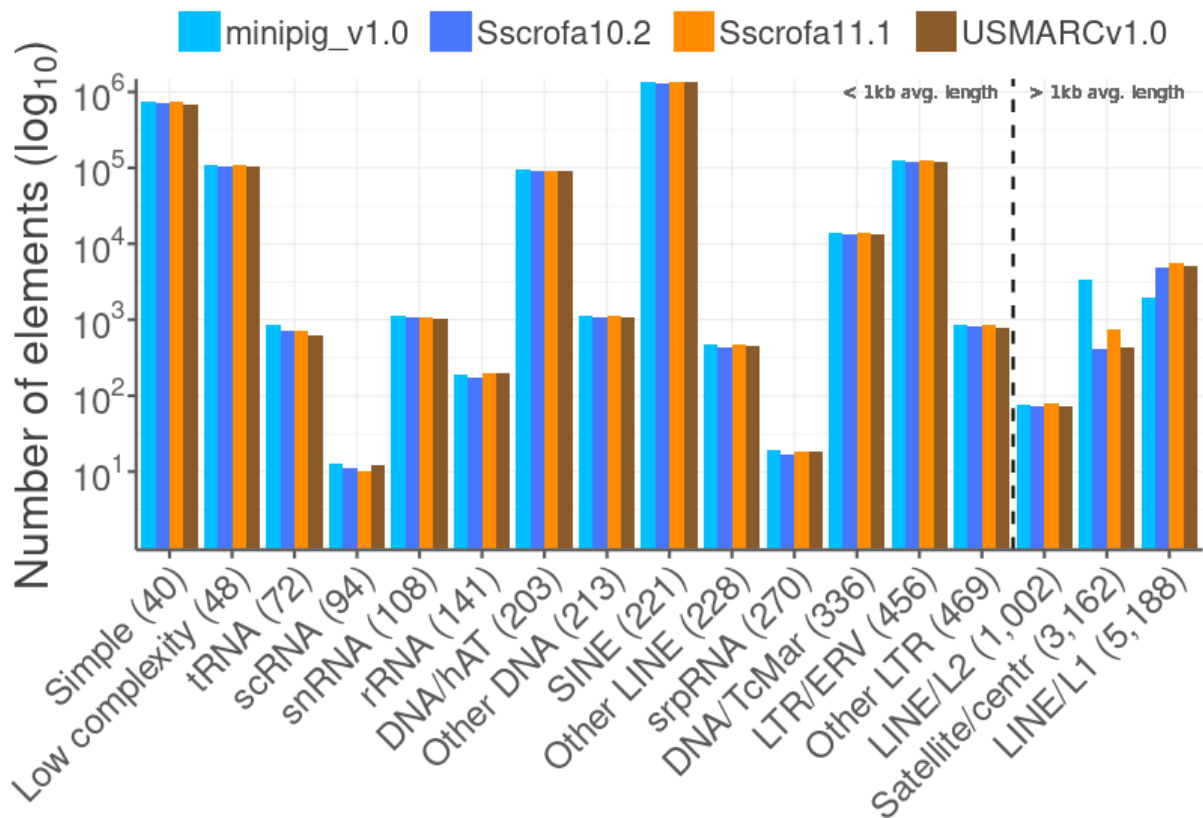
413 **Supplementary Figure SF6c:** Assemblytics comparison of USMARCv1.0 (query) against
414 the Sscrofa11.1 (reference) i). (left hand panel) variants from 50 to 500 bp; ii). (right hand
415 panel) variants from 500 to 10,000 bp.

416

417 **2. Analyses**

418 **2.1 Repeat analysis**

419 Repeats were identified using RepeatMasker (v.4.0.7) (Smit et al. 2013) with a combined
420 repeat database including Dfam (v.20170127) (Hubley *et al.*, 2016) and RepBase
421 (v.20170127) (Bao, Kojima and Kohany, 2015) on the minipig_v1.0, Sscrofa10.2,
422 Sscrofa11.1 and USMARCv1.0 assemblies. RepeatMasker was run with “sensitive” (-s)
423 setting using *sus scrofa* as the query species (-- species “*sus scrofa*”). Repeats which
424 showed greater than 40% sequence divergence or were shorter than 70% of the expected
425 sequence length were filtered out from subsequent analyses. The presence of potentially
426 novel repeats was assessed by RepeatMasker using the novel repeat library generated by
427 RepeatModeler (v.1.0.11) (Smit and Hubley, 2008).
428 The numbers of the different repeat classes and the average mapped lengths of the
429 repetitive elements identified in these four pig genome assemblies are summarised in
430 Supplementary Figures SF7 and SF8 respectively.



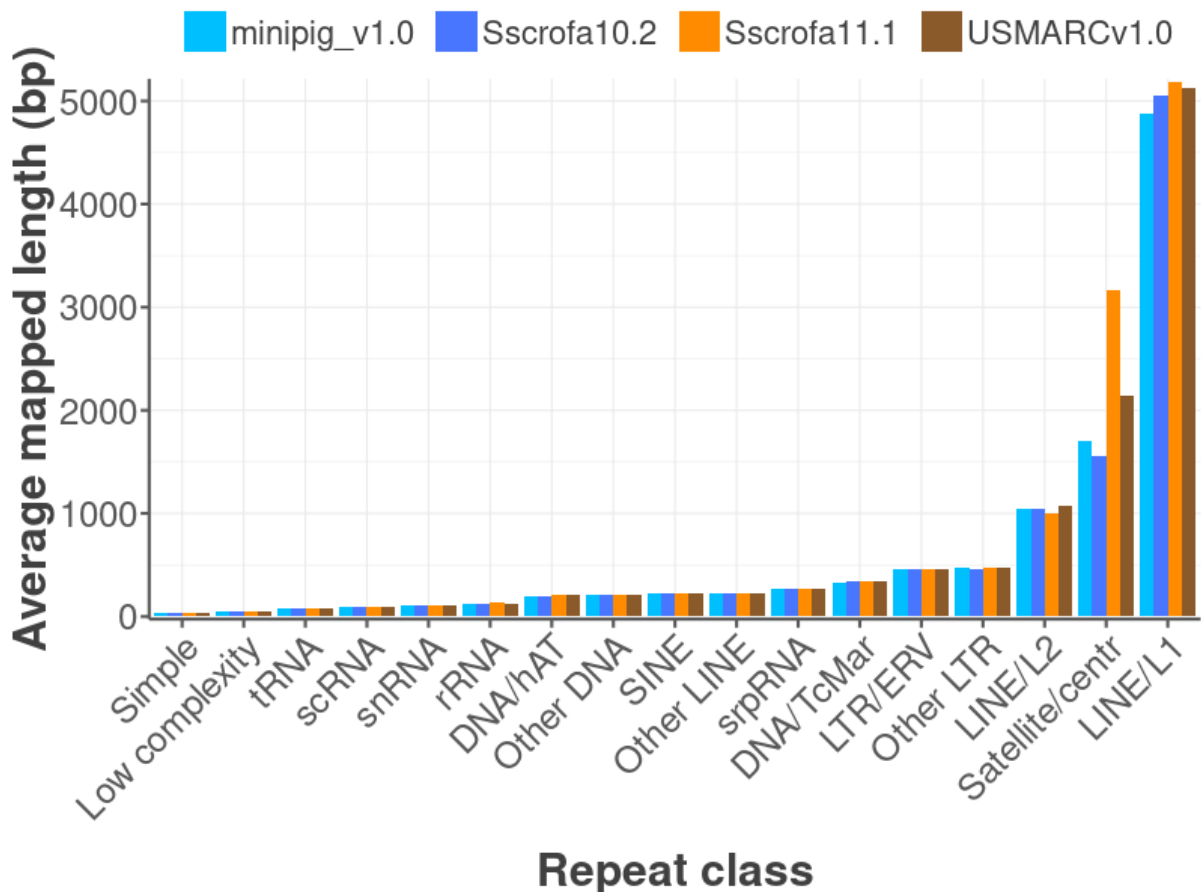
Repeat class (repeat length in bp)

431

432 **Supplementary Figure SF7:** Counts of repetitive elements in four pig assemblies. Counts

433 are given for repeat classes for which percent divergence was less than 40% and mapped

434 length was above 70% relative to the RepBase database entries.



435

436 **Supplementary Figure SF8:** Average mapped length of repetitive elements in four pig
 437 genomes.

438 **2.1.1 Telomeres**

439 Telomeres were identified by running Tandem Repeat Finder (TRF) (Benson, 1999) with
 440 default parameters apart from Mismatch (5) and Minscore (40). The identified repeat
 441 sequences were then searched for the occurrence of five identical, consecutive units of the
 442 TTAGGG vertebrate motif or its reverse complement and total occurrences of this motif was
 443 counted within the tandem repeat. Regions which contained at least 200 identical hexamer
 444 units, were >2kb of length and had a hexamer density of >0.5 were retained as potential
 445 telomeres (Supplementary Table ST5; Supplementary Figure SF9). As chromosomes SSC1-
 446 SSC12 inclusive are metacentric we would have expected to identify telomeric sequences
 447 on the short arms of these chromosomes.

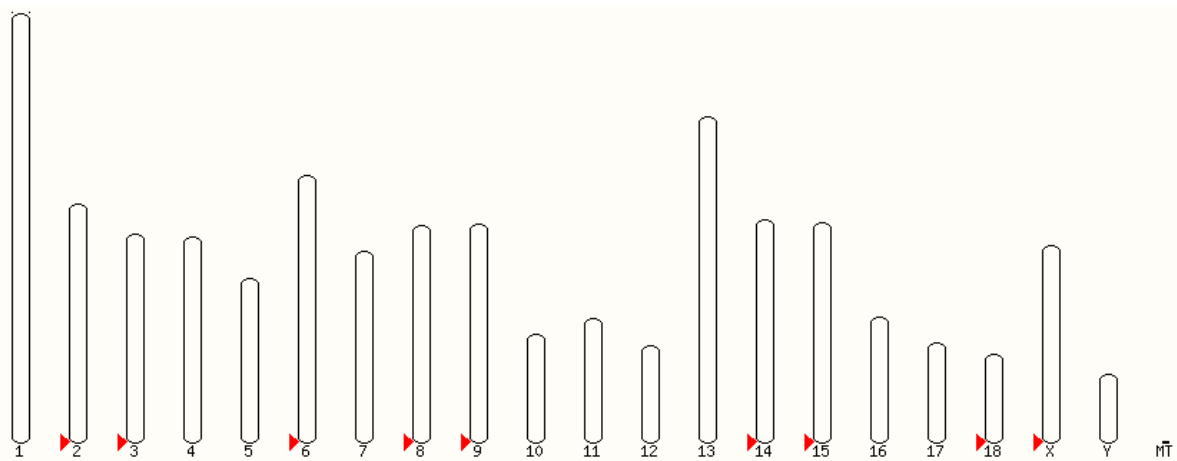
448

449

450 **Supplementary Table ST5:** Predicted telomere locations in the Sscrofa11.1 assembly.
 451 Number of exact matches of the vertebrate TTAGGG repeat sequence was used to identify
 452 candidate telomeres.

Chr	Start	End	Number of hexamers	Region length (kb)	Strand	Hexamer content
2	151,924,806	151,935,981	1,609	11.2	+	86.4%
3	132,840,959	132,848,913	1,046	8.0	+	78.9%
6	170,835,933	170,843,587	957	7.7	+	75.0%
8	138,963,948	138,966,197	208	2.2	+	55.5%
9	139,499,115	139,512,083	1,836	13.0	+	84.9%
14	141,745,369	141,755,446	1,201	10.1	+	71.5%
15	140,408,314	140,412,713	595	4.4	+	81.2%
18	55,971,782	55,982,971	1,571	11.2	+	84.2%
X	125,929,106	125,939,592	1,329	10.5	+	76.0%

453



454

455 **Supplementary Figure SF9:** Predicted locations of telomeres in the Sscrofa11.1 assembly

456 2.1.2 Centromeres

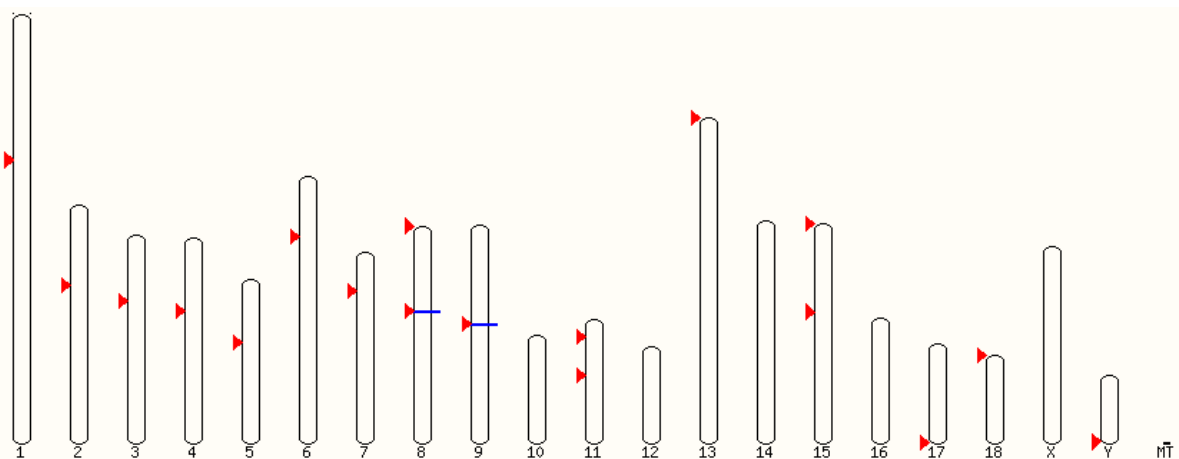
457 Centromeres were predicted using the following strategy. First, the RepeatMasker output,
 458 both default and novel, was searched for centromeric repeat occurrences. Second, the
 459 assemblies were searched for known, experimentally verified, centromere specific repeats
 460 (Miller, Hindkjær and Thomsen, 1993) (Riquet et al., 1996) in the Sscrofa11.1 genome. Then
 461 the three sets of repeat annotations were merged together with BEDTools (Quinlan and Hall,
 462 2010) (median and mean length: 786 bp and 5775 bp, respectively) and putative centromeric
 463 regions closer than 500 bp were collapsed into longer super-regions. Regions which were

464 >5kb were retained as potential centromeric sites (Supplementary Table ST6;
 465 Supplementary Figure SF10).

466 **Supplementary Table ST6:** Predicted centromere locations in the Sscrofa11.1 assembly

Chr	Start	End	Repeat content (bp)	Region length (bp)	Repeat content
1	92,615,481	92,672,216	46,164	56,735	81.4%
1	92,760,768	92,881,119	110,990	120,351	92.2%
1	93,266,464	93,430,514	80,940	16,4050	49.3%
2	50,550,173	50,777,308	198,336	227,135	87.3%
3	41,776,737	41,860,603	35,376	83,866	42.2%
4	46,443,460	46,472,085	28,625	28,625	100.0%
5	39,774,025	39,828,563	54,538	54,538	100.0%
5	39,878,566	40,207,105	328,539	328,539	100.0%
6	38,712,705	38,886,534	163,335	173,829	94.0%
7	24,578,125	24,606,761	28,636	28,636	100.0%
8	144	20,905	20,761	20,761	100.0%
8	54,585,508	54,685,241	21,099	99,733	21.2%
9	63,144,551	63,503,859	356,770	359,308	99.3%
11	11,220,831	11,222,126	1,295	1,295	100.0%
11	35,726,738	35,728,355	1,617	1,617	100.0%
11	35,804,210	35,809,503	5,293	5,293	100.0%
11	35,870,705	35,878,206	7,501	7,501	100.0%
13	34	152,474	150,375	152,440	98.6%
15	1,649	36,105	10,369	34,456	30.1%
15	56,407,100	56,427,869	9,798	20,769	47.2%
17	63,189,675	63,361,433	171,758	171,758	100.0%
18	619	17,212	16,593	16,593	100.0%
Y	42,496,777	42,515,903	17,954	19,126	93.9%

467



468

469 **Supplementary Figure SF10:** Predicted centromere locations in the Sscrofa11.1 assembly.

470

471

472 **2.2 Transcriptome data used for building gene models**

473 Two new sources of transcriptome sequence data were generated for use in building gene
474 models as described below – Annotation (Ensembl). First, long read transcript data (Iso-Seq)
475 were generated on the Pacific Bioscience RSII platform. Second, short read Illumina RNA-
476 Seq data.

477 **2.2.1 Iso-Seq**

478 The following tissues were harvested from MARC1423004 at age 48 days: brain
479 (BioSamples: SAMN05952594), diaphragm (SAMN05952614), hypothalamus
480 (SAMN05952595), liver (SAMN05952612), small intestine (SAMN05952615), skeletal
481 muscle – *longissimus dorsi* (SAMN05952593), spleen (SAMN05952596), pituitary
482 (SAMN05952626) and thymus (SAMN05952613).

483 Total RNA from each of these tissues was extracted using Trizol reagent (ThermoFisher
484 Scientific) and the provided protocol. Briefly, approximately 100 mg of tissue was ground in a
485 mortar and pestle cooled with liquid nitrogen, and the powder was transferred to a tube with
486 1 ml of Trizol reagent added and mixed by vortexing. After 5 minutes at room temperature,
487 0.2 mL of chloroform was added and the mixture was shaken for 15 seconds and left to
488 stand another 3 minutes at room temperature. The tube was centrifuged at 12,000 x g for
489 15 minutes at 4°C. The RNA was precipitated from the aqueous phase with 0.5 mL of
490 isopropanol. The RNA was further purified with extended DNase I digestion to remove
491 potential DNA contamination. The RNA quality was assessed with a Fragment Analyzer
492 (Advanced Analytical Technologies Inc., IA). Only RNA samples of RQN above 7.0 were
493 used for library construction. PacBio IsoSeq libraries were constructed per the PacBio
494 IsoSeq protocol. Briefly, starting with 3 µg of total RNA, cDNA was synthesized by using
495 SMARTer PCR cDNA Synthesis Kit (Clontech, CA) according to the IsoSeq protocol (Pacific
496 Biosciences, CA). Then the cDNA was amplified using KAPA HiFi DNA Polymerase (KAPA
497 Biotechnologies) for 10 or 12 cycles followed by purification and size selection into 4
498 fractions: 0.8-2 kb, 2-3 kb, 3-5 kb and >5 kb. The fragment size distribution was validated on
499 a Fragment Analyzer (Advanced Analytical Technologies Inc, IA) and quantified on a DS-11

500 FX fluorometer (DeNovix, DE). After a second round of large scale PCR amplification and
501 end repair, SMRT bell adapters were separately ligated to the cDNA fragments. Each size
502 fraction was sequenced on 4 or 5 SMRT Cells v3 using P6-C4 chemistry and 6 hour movies
503 on a PacBio RS II sequencer (Pacific Bioscience, CA). Short read RNA-Seq libraries were
504 also prepared for all nine tissue using TruSeq stranded mRNA LT kits and supplied protocol
505 (Illumina, CA), and sequenced on a NextSeq500 platform using v2 sequencing chemistry to
506 generate 2 x 75 bp paired-end reads.

507 **2.2.1.1 Error-correction and redundancy reduction of PacBio Iso-Seq full-length cDNA** 508 **reads**

509 The Read of Insert (ROI) were determined by using *consensustools.sh* in the SMRT-
510 Analysis pipeline v2.0, with reads which were shorter than 300 bp and whose predicted
511 accuracy was lower than 75% removed. Full-length, non-concatemer (FLNC) reads were
512 identified by running the *classify.py* command. The cDNA primer sequences as well as the
513 poly(A) tails were trimmed prior to further analysis. Paired-end Illumina RNA-Seq reads from
514 each tissue sample were trimmed to remove the adaptor sequences and low-quality bases
515 using Trimmomatic (v0.32) (Bolger, Lohse and Usadel, 2014) with explicit option settings:
516 *ILLUMINACLIP:adapters.fa: 2:30:10:1:true LEADING:3 TRAILING:3 SLIDINGWINDOW:*
517 *4:20 LEADING:3 TRAILING:3 MINLEN:25*, and overlapping paired-end reads were merged
518 using the PEAR software (v0.9.6) (Zhang *et al.*, 2014). Subsequently, the merged and
519 unmerged RNA-Seq reads from the same tissue samples were *in silico* normalized in a
520 mode for single-end reads by using a Trinity (v2.1.1) (Grabherr *et al.*, 2011) utility,
521 *insilico_read_normalization.pl*, with the following settings: *--max_cov 50 --max_pct_stdev*
522 *100 --single*. Errors in the full-length, non-concatemer reads were corrected with the
523 preprocessed RNA-Seq reads from the same tissue samples by using *proofread* (v2.12)
524 (Hackl *et al.*, 2014). Untrimmed sequences with at least some regions of high accuracy in
525 the *.trimmed.fq* files were extracted based on sequence IDs in *.untrimmed.fa* files to balance
526 off the contiguity and accuracy of the final reads.

527 **2.2.2 RNA-Seq**

528 In addition to the Illumina short read RNA-seq data generated from MARC1423004 and used
 529 to correct the Iso-Seq data (see above), Illumina short read RNA-seq data (PRJEB19386)
 530 were also generated from a range of tissues from four juvenile Duroc pigs (two male, two
 531 female) and used for annotation as described below. Extensive metadata with links to the
 532 protocols for sample collection and processing are linked to the BioSample entries under the
 533 Study Accession PRJEB19386. The tissues sampled are listed in Supplementary Table ST7.
 534 Sequencing libraries were prepared using a ribodepletion TruSeq stranded RNA protocol
 535 and 150 bp paired end sequences generated on the Illumina HiSeq 2500 platform in rapid
 536 mode.

537 **Supplementary Table ST7:** Tissue samples characterised by Illumina short read RNA-Seq
 538 analyses

Tissue	BioSample accession	alias	Animal	Sex
alveolar macrophages	SAMEA103886124	SUS_RI_DUR21-30	Duroc 21	female
alveolar macrophages	SAMEA103886168	SUS_RI_Pig 21_DUR_30	Duroc 21	female
alveolar macrophages	SAMEA103886137	SUS_RI_DUR22-60	Duroc 22	male
alveolar macrophages	SAMEA103886112	SUS_RI_Pig 22_DUR_60	Duroc 22	male
amygdala	SAMEA103886173	SUS_RI_R-Dur_23-08	Duroc 23	female
amygdala	SAMEA103886162	SUS_RI_Dur_24-C-S0	Duroc 24	male
brain, frontal lobe	SAMEA103886139	SUS_RI_R-Dur_23-01	Duroc 23	female
brain, frontal lobe	SAMEA103886156	SUS_RI_R-Dur_24-41	Duroc 24	male
brain stem	SAMEA103886128	SUS_RI_R-Dur_23-05	Duroc 23	female
brain stem	SAMEA103886129	SUS_RI_R-Dur_24-45	Duroc 24	male
caecum	SAMEA103886133	SUS_RI_DUR21-19	Duroc 21	female
caecum	SAMEA103886120	SUS_RI_DUR22-48	Duroc 22	male
caecum	SAMEA103886151	SUS_RI_Pig 22_DUR_48	Duroc 22	male
cerebellum	SAMEA103886116	SUS_RI_R-Dur_23-09	Duroc 23	female
cerebellum	SAMEA103886131	SUS_RI_R-Dur_24-49	Duroc 24	male
colon	SAMEA103886132	SUS_RI_Dur_23-21	Duroc 23	female
colon	SAMEA103886147	SUS_RI_Dur_24-61	Duroc 24	male
corpus callosum	SAMEA103886154	SUS_RI_R-Dur_23-10	Duroc 23	female
corpus callosum	SAMEA103886167	SUS_RI_R-Dur_24-50	Duroc 24	male
duodenum	SAMEA103886155	SUS_RI_Dur_23-22	Duroc 23	female

Tissue	BioSample accession	alias	Animal	Sex
duodenum	SAMEA103886176	SUS_RI_Dur_24-62	Duroc 24	male
epididymis	SAMEA103886140	SUS_RI_DUR22-58	Duroc 22	male
hippocampus	SAMEA103886122	SUS_RI_Dur_23-B-S0	Duroc 23	female
hippocampus	SAMEA103886114	SUS_RI_R-Dur_24-51	Duroc 24	male
ileum	SAMEA103886163	SUS_RI_Dur_23-23	Duroc 23	female
ileum	SAMEA103886121	SUS_RI_Dur_24-63	Duroc 24	male
kidney cortex	SAMEA103886174	SUS_RI_DUR21-09	Duroc 21	female
kidney cortex	SAMEA103886153	SUS_RI_DUR22-39	Duroc 22	male
heart, left ventricle	SAMEA103886169	SUS_RI_DUR21-12	Duroc 21	female
heart, left ventricle	SAMEA103886172	SUS_RI_DUR22-43	Duroc 22	male
lymph node, mesenteric	SAMEA103886127	SUS_RI_DUR21-22	Duroc 21	female
lymph node, mesenteric	SAMEA103886115	SUS_RI_DUR22-51	Duroc 22	male
medulla oblongata	SAMEA103886135	SUS_RI_R-Dur_23-06	Duroc 23	female
medulla oblongata	SAMEA103886142	SUS_RI_R-Dur_24-46	Duroc 24	male
occipital lobe	SAMEA103886158	SUS_RI_R-Dur_23-02	Duroc 23	female
occipital lobe	SAMEA103886177	SUS_RI_R-Dur_24-42	Duroc 24	male
omentum	SAMEA103886145	SUS_RI_DUR21-65	Duroc 21	female
omentum	SAMEA103886146	SUS_RI_DUR22-73	Duroc 22	male
penis	SAMEA103886166	SUS_RI_DUR22-59	Duroc 22	male
pituitary gland	SAMEA103886152	SUS_RI_Dur_23-14	Duroc 23	female
pituitary gland	SAMEA103886150	SUS_RI_Dur_24-54	Duroc 24	male
pituitary gland	SAMEA103886149	SUS_RI_DUR21-06	Duroc 21	female
pons	SAMEA103886159	SUS_RI_R-Dur_23-07	Duroc 23	female
pons	SAMEA103886164	SUS_RI_R-Dur_24-47	Duroc 24	male
skeletal muscle	SAMEA103886171	SUS_RI_DUR21-24	Duroc 21	female
skeletal muscle	SAMEA103886118	SUS_RI_DUR22-75	Duroc 22	male
spleen	SAMEA103886157	SUS_RI_DUR21-25	Duroc 21	female
spleen	SAMEA103886170	SUS_RI_DUR22-55	Duroc 22	male
stomach	SAMEA103886111	SUS_RI_Dur_23-24	Duroc 23	female
stomach	SAMEA103886134	SUS_RI_Dur_24-64	Duroc 24	male
thalamus	SAMEA103886136	SUS_RI_R-Dur_23-13	Duroc 23	female
thalamus	SAMEA103886160	SUS_RI_R-Dur_24-53	Duroc 24	male
tonsils	SAMEA103886125	SUS_RI_DUR22-56	Duroc 22	male
uterus	SAMEA103886126	SUS_RI_DUR21-27	Duroc 21	female

540 **2.3 SNP chip variants**

541 **2.3.1 SNP chip probes mapped to assemblies**

542 The probes from four commercial SNP chips were mapped to the Sscrofa10.2, Sscrofa11.1
543 and USMARCv1.0 assemblies using BWA MEM (Li and Durbin, 2009) and a wrapper script
544 (https://github.com/njdbickhart/perl_toolchain/blob/master/assembly_scripts/alignAndOrderSnpProbes.pl).

- 546 • Illumina PorcineSNP60 ((Ramos *et al.*, 2009), <https://emea.illumina.com/products/by-type/microarray-kits/porcine-snp60.html>)
- 548 • Affymetrix Axiom™ Porcine Genotyping Array
549 (<https://www.thermofisher.com/order/catalog/product/550588>)
- 550 • Gene Seek Genomic Profiler Porcine – HD beadChip
551 (<http://genomics.neogen.com/uk/ggp-porcine>)
- 552 • Gene Seek Genomic Profiler Porcine v2– LD Chip
553 (<http://genomics.neogen.com/uk/ggp-porcine>)

554 Probe sequence was derived from the marker manifest files that are available on the
555 provider websites. In order to retain marker manifest coordinate information, each probe
556 marker name was annotated with the chromosome and position of the marker's variant site
557 from the manifest file. All mapping coordinates were tabulated into a single file, and were
558 sorted by the chromosome and position of the manifest marker site. In order to derive and
559 compare relative marker rank order, a custom Perl script
560 (https://github.com/njdbickhart/perl_toolchain/blob/master/assembly_scripts/pigGenomeSNP_SortRankOrder.pl)
561 was used to sort and number markers based on their mapping locations
562 in each assembly.

563 A Spearman's rank order (ρ) value was calculated for each assembly (alternative
564 hypothesis: ρ is equal to zero; $p < 2.2 \times 10^{-16}$) (Supplementary Table ST9). This rank order
565 comparison was estimated by ordering all of the SNP probes from all chips by their listed
566 manifest coordinates against their relative order in each assembly (with chromosomes
567 ordered by karyotype). Any unmapped markers in an assembly were penalized by giving the

568 marker a "-1" rank in the assembly ranking order. The methods are similar to what those
 569 used to assess the relative order of the ARS1 Goat assembly RH map vs the scaffold order
 570 ((Bickhart *et al.*, 2017) see Supplementary Note 1).

571

572 **Supplementary Table ST8:** SNP chip markers mapped to pig genome assemblies

Assembly	Mapped / unmapped	AxiomHD	PorcineSNP60	GGP LD	80K
Sscrofa10.2	mapped	633,705	59,590	50,530	68,046
	unmapped	24,987	1,975	385	470
Sscrofa11.1	mapped	628,280	61,299	50,586	68,270
	unmapped	30,412	266	329	246
USMARCv1.0	mapped	618,771	60,692	50,042	67,604
	unmapped	39,921	873	873	912

573

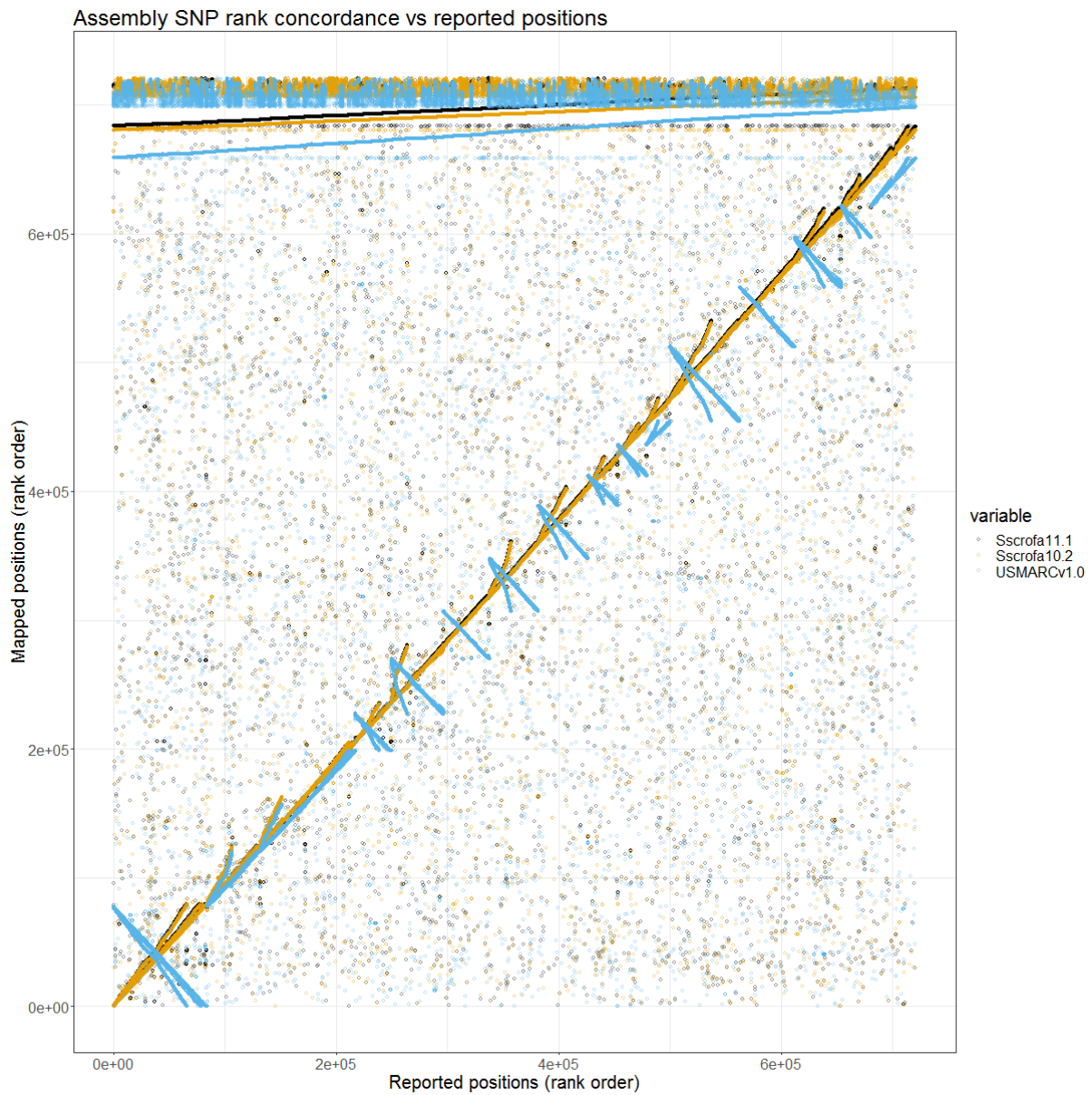
574 **Supplementary Table ST9:** Spearman's rank order

Assembly	Rho
Sscrofa10.2	0.88464
Sscrofa11.1	0.88890
USMARCv1.0	0.81260

575

576 In order to examine general linear order of placed markers on each assembly, the marker
 577 rank order (y axis; used above in the Spearman's rank order test) was plotted against the
 578 rank order of the probe rank order on the manifest file (x axis) (Supplementary Figure SF11).

579 **Supplementary Figure SF11:** Assembly SNP rank concordance versus reported
580 chromosomal location



581
582 The analyses reveal some interesting artifacts that suggest that the SNP manifest
583 coordinates for the porcine 60K SNP chip are still derived from an obsolete (Sscrofa9)
584 reference in contrast to all other manifests (Sscrofa10.2). Also, it confirms that several of the
585 USMARCv1.0 chromosome scaffolds are inverted with respect to the canonical orientation of
586 pig chromosomes. Such inversions are due to the agnostic nature of genome assembly and
587 post-assembly polishing programs. Unless these are corrected post-hoc by manual curation,
588 they result in artefactual inversions of the entire chromosome. However, such inversions do

589 not generally impact downstream analysis that does not involve the relative order/orientation
590 of whole chromosomes. The large band of points at the top of the plot corresponds to marker
591 mappings on the unplaced contigs of each assembly. These unplaced contigs often
592 correspond to assemblies of alternative haplotypes in heterozygous regions of the reference
593 animal (Koren *et al.*, 2018). Marker placement on these segments suggests that these
594 variants are tracking different haplotypes in the population, which is the desired intent of
595 genetic markers used in Genomic Selection.

596 **3. Annotation (Ensembl)**

597 **3.1 Repeat Finding**

598 After loading into a database, the Sscrofa11.1. genomic sequence was screened for
599 sequence patterns, including repeats using RepeatMasker (Smit *et al.*, 2013-5) (version
600 4.0.5) with parameters '-nolow -species "sus scrofa" -engine "crossmatch"', dustmasker
601 (Camacho *et al.*, 2009) and TRF (Benson, 1999). Both executions of RepeatMasker and
602 dustmasker combined masked 45.04% of the assembly.

603 **3.2 Raw computes**

604 Transcription start sites (TSS) were predicted using Eponine-scan (Down and Hubbard,
605 2002). CpG islands [Micklem, G., unpublished] longer than 400 bases and tRNAs (Lowe and
606 Eddy, 1996) were also predicted. The results of Eponine-scan, CpG and tRNAscan are for
607 display purposes only and are not used subsequently in the gene annotation process.

608 Genscan (Burge and Karlin, 1997) was run across the repeat-masked sequence and the
609 results were used as input for UniProt (Goujon *et al.*, 2010), UniGene (Sayers *et al.*, 2010)
610 and Vertebrate RNA (www.ebi.ac.uk/ena/) alignments by BLAST+ (Camacho *et al.*, 2009).

611 Passing only Genscan results to BLAST is an effective way of reducing the search space
612 and therefore the computational resources required. The resulting alignments to the
613 Sscrofa11.1 assembly included 5,680,769 UniProt, 4,801,230 UniGene and 4,414,040
614 Vertebrate RNA sequences.

615 **3.3 Generation of gene models**

616 Various sources of transcript and protein data were investigated and used to generate gene
617 models using a variety of techniques and are outlined here. The number of gene models
618 generated are summarised in Table ST10.

619 **Table ST10:** Gene model generation overview

Pipeline	Source	Number of models
Species specific cDNAs	RefSeq, ENA	45,589
PacBio Iso-Seq	USDA MARC	326,217
RNA-Seq	The Roslin Institute	572,419
Olfactory receptors	Human and mouse Ensembl Release 89	1,212
IG/TR genes	IMGT®	1,803
Protein-to-genome	Subset of UniProt vertebrate proteins	509,769

620

621 **3.3.1 cDNA alignments**

622 Pig cDNAs were downloaded from ENA and RefSeq, and aligned to the Sscrofa11.1
623 assembly using Exonerate (Slater and Birney, 2005). A minimal sequence length of 60 bp
624 was used and a cut-off of 97% identity and 90% coverage were required for an alignment to
625 be processed further. The cDNAs are mainly used for display purposes, but can be used to
626 add untranslated regions (UTRs) to the protein coding transcript models if they have
627 matching introns.

628 **Table ST11:** Species specific cDNAs aligned against Sscrofa11.1

Species	Initial mRNA sequences	Sequences aligned
Pig	45,571	45,526

629

630 **3.3.2 PacBio Iso-Seq transcript data**

631 PacBio Iso-Seq data are high coverage long read transcriptomic data that allows for
632 correction for the high error rate in raw PacBio reads. The consensus sequences
633 representing nine tissues (brain, diaphragm, hypothalamus, liver, skeletal muscle
634 (*longissimus dorsi*), pituitary, small intestine, spleen, and thymus were downloaded from the

635 short read archive (SRA: PRJNA351265) after correction using Illumina short reads from the
 636 same tissue type. The sequences were aligned to the genome using Exonerate (Slater and
 637 Birney, 2005) using a cut-off of 95% identity and 90% coverage. All the Iso-Seq data sets
 638 had 3' capping and were used for adding UTRs to homology-based protein coding models.
 639 All Iso-Seq data sets were used as lincRNA candidates for our lincRNA prediction pipeline.

640 **Table ST12:** PacBio Iso-Seq sequences aligned against Sscrofa11.1

Tissue sample	Initial Iso-Seq sequences	Aligned sequences
Liver	588,957	491,796
Thymus	567,700	374,515
Hypothalamus	414,021	256,930
Brain	398,629	354,494
Skeletal muscle (<i>l. dorsl</i>)	410,420	361,494
Diaphragm	459,911	391,813
Spleen	674,053	449,425
Pituitary	411,562	252,707
Small intestine	494,538	406,144

641

642 3.3.3 Protein-to-genome alignment

643 Protein sequences were downloaded from UniProt and aligned to the Sscrofa11.1 assembly
 644 in a splice aware manner using GenBlast (She *et al.*, 2011). The set of proteins aligned to
 645 the genome was a subset of UniProt proteins used to provide a broad targeted coverage of
 646 the pig genome. The set consisted of the following:

- 647 • Pig PE level 1, 2, 3
- 648 • Human PE level 1, 2, 3
- 649 • Mouse PE level 1, 2, 3
- 650 • Other mammals PE level 1, 2, 3
- 651 • Other vertebrates PE level 1, 2, 3

652 Note: PE level = protein existence level A cut-off of 50 percent coverage and identity and an
 653 e-value of e^{-1} were used for GenBlast (She *et al.*, 2011) with the exon repair option turned
 654 on. The top 5 transcript models built by GenBlast for each protein passing the cut-offs were
 655 kept. This process produced 509,769 transcript models in total.

656 **3.3.4 RNA-seq pipeline**

657 RNA-Seq data downloaded from ENA PRJEB19386 were used in the annotation. These
658 RNA-Seq data consisted of 150 bp paired end reads from libraries prepared using a
659 stranded library protocol from ribo-depleted total RNA from Duroc pigs. The dataset
660 comprised RNA-Seq data from 28 tissue and cell samples: alveolar macrophages,
661 amygdala, brain stem, caecum, cerebellum, colon, corpus callosum, duodenum, epididymis,
662 frontal lobe (brain), hippocampus, ileum, kidney cortex, left ventricle (heart), mesenteric
663 lymph node, medulla oblongata, occipital lobe, omentum, penis, pituitary gland, pons,
664 skeletal muscle, spleen, stomach, thalamus, tonsil, uterus (Supplementary Table ST7). A
665 merged file containing reads from all tissues was also created. The merged data was less
666 likely to suffer from model fragmentation due to read depth. The available reads were
667 aligned to the Sscrofa11.1 assembly using BWA. A 50 percent allowed mismatch criteria
668 was applied to identify potential splice junctions. Initial rough exon/intron boundaries were
669 generated via the BWA alignments and then refined by mapping the reads in a splice-aware
670 manner using Exonerate (Slater and Birney, 2005). The split reads and the processed BWA
671 alignments were combined to produce 1,060,366 transcript models in total. The predicted
672 open reading frames were compared to UniProt proteins using NCBI BLAST. Models with
673 poorly scoring or no BLAST alignments were split into a separate class and considered as
674 potential lincRNAs.

675

676 **Supplementary Table ST13:** Tissue-specific values for initial read counts along with the
677 percent of mapped and properly paired reads. The final column shows the count of potential
678 transcript models build per tissue.

Tissue name	Total reads	Mapped	Properly paired	Transcript models
Alveolar macrophages	508,512,918	92.69%	64.31%	34,867
Amygdala	170,434,766	93.73%	64.43%	38,118
Brain stem	124,538,342	93.33%	61.60%	35,791
Caecum	444,611,528	92.40%	71.78%	40,716
Cerebellum	158,560,324	94.09%	64.42%	36,132
Colon	168,263,230	90.80%	61.79%	34,520
Corpus callosum	148,039,874	93.75%	62.68%	37,474
Duodenum	346,909,970	91.94%	62.08%	40,112
Epididymis	186,743,514	92.74%	69.27%	37,377
Frontal lobe	119212918	94.30%	59.99%	35,119
Hippocampus	164,637,176	94.72%	62.38%	36,403
Ileum	166,645,682	91.96%	69.83%	36,661
Kidney cortex	258,616,430	95.30%	86.38%	35,544
Left ventricle	265,075,268	95.33%	86.11%	33,125
Mesenteric lymph node	448,893,104	93.24%	69.37%	40,250
Medulla oblongata	141,361,800	93.18%	58.96%	42,716
Occipital lobe	13,3884,172	94.23%	64.25%	35,390
Omentum	179,713,086	93.70%	84.61%	27,570
Penis	179,834,564	93.15%	71.84%	37,121
Pituitary	164,402,132	93.64%	61.23%	35,482
Pituitary gland	131,196,396	95.15%	86.44%	33,800
Pons	134,913,426	93.80%	61.90%	35,974
Skeletal muscle	206,977,278	92.09%	81.55%	32,011
Spleen	194,924,210	94.26%	83.52%	35,130
Stomach	141,172,602	92.49%	70.72%	33,326
Thalamus	149,227,654	93.84%	53.67%	36,047
Tonsil	320,766,440	94.22%	74.78%	38,154
Uterus	90,381,988	94.56%	59.49%	31,178

679

680 **3.3.5 IG and TR genes**

681 All pig, cow, sheep, human and mouse IG/TR V, C and J segment protein sequences were
682 downloaded from IMGT® (Lefranc *et al.*, 2015) and aligned against the Sscrofa11.1
683 assembly using Exonerate (Slater and Birney, 2005) using ‘—max-intron 50000’ and only the
684 models with 95% coverage and 80% identity were kept. We generated 1,803 gene models.
685 For positions where there were overlapping transcript models, the transcript model with the
686 highest combined alignment coverage and percent identity was kept as the representative
687 model for the locus.

688 **3.3.6 Olfactory receptor genes**

689 We used the manually curated human and mouse set (Ensembl release 89) and pig
690 olfactory receptor sequences (Nguyen *et al.*, 2012). The sequences were aligned against the
691 genome with Exonerate (Slater and Birney, 2005) and only the models with high similarity
692 (95% coverage, 95% identity) were kept, yielding 1,212 gene models.

693 **3.3.7 Selenocysteine proteins**

694 Known selenocysteine proteins were aligned against the Sscrofa11.1 assembly using
695 Exonerate (Slater and Birney, 2005). The models generated were checked for the presence
696 of selenocysteines in the same positions as the known proteins. We generated 103 models.

697 **3.3.8 Filtering the models**

698 The filtering phase decided the subset of protein-coding transcript models, generated from
699 the model-building pipelines, that would comprise the final protein-coding gene set in the
700 GeneBuild. Models were filtered based on information such as what pipeline they were
701 generated using, how closely related the data are to the target species (i.e. pig) and how
702 good the alignment coverage and percent identity to the original data are. Models were
703 filtered using the LayerAnnotation and GeneBuilder modules. The Apollo software (Lewis *et*
704 *al.*, 2002) was used to visualise the results of the filtering.

705 **3.3.9 Collapsing the transcript set**

706 The LayerAnnotation module was used to define a hierarchy of input data sets, from most
707 preferred to least preferred. The output of this pipeline included all transcript models from the

708 highest ranked input set. Models from the lower ranked input sets are included only if their
709 exons do not overlap a model from an input set higher in the hierarchy. Note that models
710 cannot exist in more than one layer. For UniProt proteins, models were also separated into
711 clades. To help selection during the layering process. Each UniProt protein was in one clade
712 only, for example mammal proteins were present in the mammal clade and were not present
713 in the vertebrate clade to avoid aligning the proteins multiple times.

714 Layer 1:

- 715 • Pig seleno-proteins
- 716 • Pig olfactory receptors with $\geq 90\%$ coverage and 97% identity
- 717 • All vertebrate seleno-proteins with full RNA-seq support
- 718 • IG and TR genes

719 Layer 2:

- 720 • Pig cDNA models with $\geq 90\%$ coverage and 97% identity
- 721 • Pig IsoSeq models with protein support $\geq 80\%$ coverage and identity and full RNA-
722 seq support
- 723 • RNA-seq models with $\geq 95\%$ coverage and identity
- 724 • Pig curated UniProt proteins from PE levels 1 & 2 with $\geq 80\%$ coverage and identity
725 and full RNA-seq support
- 726 • Pig curated UniProt proteins from PE levels 3 with $\geq 95\%$ coverage and identity and
727 full RNA-seq support
- 728 • All vertebrate curated UniProt proteins from PE levels 1 & 2 with $\geq 95\%$ coverage
729 and identity and full RNA-seq support

730 Layer 3:

- 731 • RNA-seq models with $\geq 80\%$ coverage and identity

732 Layer 4:

- 733 • Pig curated UniProt proteins from PE levels 1 & 2 with $\geq 50\%$ coverage and identity
- 734 • Pig IsoSeq models with protein support $\geq 80\%$ coverage and identity

735 Layer 5:

- 736 • Pig curated UniProt proteins from PE levels 3 with $\geq 80\%$ coverage and identity
- 737 • All vertebrate curated UniProt proteins from PE levels 1 & 2 with $\geq 80\%$ coverage
- 738 and identity

739 Layer 6:

- 740 • RNA-seq models with $\geq 50\%$ coverage and identity
- 741 • Pig IsoSeq models with protein support $\geq 50\%$ coverage and identity
- 742 • Pig curated UniProt proteins from PE levels 3 with $\geq 50\%$ coverage and identity
- 743 • All vertebrate curated UniProt proteins from PE levels 1 & 2 with $\geq 50\%$ coverage
- 744 and identity

745 Layer 7:

- 746 • Pig UniProt proteins from PE levels 1 & 2 & 3 with $\geq 80\%$ coverage and identity and
- 747 full RNA-seq support
- 748 • All vertebrate UniProt proteins from PE levels 1 & 2 with $\geq 80\%$ coverage and
- 749 identity and full RNA-seq support

750 Layer 8:

- 751 • Pig UniProt proteins from PE levels 1 & 2 & 3 with $\geq 50\%$ coverage and identity and
- 752 full RNA-seq support
- 753 • All vertebrate UniProt proteins from PE levels 1 & 2 with $\geq 50\%$ coverage and
- 754 identity and full RNA-seq support
- 755 • Pig IsoSeq models with protein support $\geq 50\%$ coverage and identity which may
- 756 have retained an intron

757 Layer 9:

- 758 • Pig UniProt proteins from PE levels 1 & 2 & 3 with $\geq 80\%$ coverage and identity
- 759 • All vertebrate UniProt proteins from PE levels 1 & 2 with $\geq 80\%$ coverage and
- 760 identity

761

762 Layer 10:

- 763 • Pig UniProt proteins from PE levels 1 & 2 & 3 with $\geq 50\%$ coverage and identity
- 764 • All vertebrate UniProt proteins from PE levels 1 & 2 with $\geq 50\%$ coverage and
765 identity

766 **3.3.10 Addition of UTR to coding models**

767 The set of coding models was extended into the untranslated regions (UTRs) using RNA-
768 seq, cDNA and Iso-Seq sequences. The source of the UTRS was prioritised with UTR
769 coming from cDNAs and Iso-Seq, then RNA-seq.

770 **3.3.11 Generating multi-transcript genes**

771 The steps described above generated a large set of potential transcript models, many of
772 which overlapped one another. Redundant transcript models were collapsed and the
773 remaining unique set of transcript models were clustered into multi-transcript gene where
774 each transcript in a gene has at least one coding exon that overlaps a coding exon from
775 another transcript within the same genes.

776 At this stage the gene set comprised 23,025 genes with 46,511 transcripts.

777 **3.3.12 Pseudogenes**

778 The Pseudogene module was run to identify pseudogenes from within the set of gene
779 models. A total of 178 genes were labelled as pseudogenes or processed pseudogenes.

780 **3.3.13 Small ncRNAs**

781 Small structured non-coding genes were added using annotations taken from RFAM
782 (Griffiths-Jones *et al.*, 2003) and miRBase (Griffiths-Jones *et al.*, 2006). BLAST+ was run for
783 these sequences and models built using the Infernal software suite (Eddy, 2002).

784 **3.3.14 lincRNAs discovery**

785 Using the transcriptomic data set, we tried to predict long intergenic non-coding RNAs
786 (lincRNAs). We used the RNA-seq and Iso-Seq data which were filtered against the protein-
787 coding gene set. Candidate lincRNAs that overlapped a protein-coding gene were discarded.
788 The Pfam analysis of InterProScan was run against the filtered gene set. Candidate
789 lincRNAs with a Pfam domain were also discarded.

790 **3.3.15 Cross-referencing and stable identifiers**

791 Before public release the transcripts and translations were given external references (cross-
 792 references to external databases). Stable identifiers were assigned to each gene, transcript,
 793 exon and translation. As earlier pig genome sequences have been annotated by Ensembl
 794 previously a comparison was made to the previous gene set and as many stable identifiers
 795 as possible were mapped between the two annotations.

796 **3.3.16 Gene expression**

797 The Illumina RNA-Seq data (Supplementary Table ST7) were also processed by the EBI
 798 Gene Expression Atlas (GXA) team (Papatheodorou *et al.*, 2018)
 799 (<https://www.ebi.ac.uk/gxa/home>) to generate a baseline gene expression atlas (Expression
 800 Atlas release 25, August 2017). These gene expression data can be visualised in the
 801 Ensembl genome browser from the gene page.

802 **3.3.17 Comparison of Ensembl and NCBI annotation**

803 The Sscrofa11.1 assembly was also annotated independently by the NCBI
 804 (https://www.ncbi.nlm.nih.gov/genome/annotation_euk/Sus_scrofa/106/). We have
 805 compared these two annotations (Supplementary Table ST14).

806 **Supplementary Table ST14: Comparison of Ensembl and NCBI annotation of Sscrofa11.1**

Ensembl		NCBI			
		missing (relative location)			
		in common	(intragenic)	(intergenic)	other
Protein-coding	22,452	18,772	270	1,785	*1,625
Non-coding	3,250	811	1,158	1,281	
Pseudogenes	178	121	1	56	
NCBI		Ensembl			
		missing (relative location)			
		in common	(intragenic)	(intergenic)	other
Protein-coding	20,790	18,772	119	1,899	
Non-coding	6,460	811	541	3,730	**1,378
Pseudogenes	3,084	121	124	1,214	*1,625

807 * 1,625 genes annotated as protein-coding by Ensembl are annotated as pseudogenes by NCBI

808 ** 1,378 genes annotated as non-coding by NCBI are annotated as protein-coding by Ensembl

809 **3.3.18 Annotation of the USMARCv1.0 assembly**

810 Annotation for USMARCv1.0 was carried out using the Ensembl pipeline and the same key
811 steps as outlined for Sscrofa11.1. To help with the consistency of annotation, the same set
812 of long and short read transcriptomic data were used in the annotation of USMARCv1.0. As
813 the annotations were done two years apart there was some variance in terms of the
814 underlying code base used to generate the annotations. We plan to update the Sscrofa11.1
815 annotation in future to take advantage of these upgrades, though the effect on the overall
816 geneset is likely to be marginal due to the amount of high quality transcriptomic data
817 available for the original annotation.

818

819 **4. References**

- 820 Anderson, S. I. *et al.* (2000) 'A large-fragment porcine genomic library resource in a BAC
821 vector', *Mammalian Genome*, 11(9), pp. 811–814. doi: 10.1007/s003350010155.
- 822 Bao, W., Kojima, K. K. and Kohany, O. (2015) 'Repbse Update, a database of repetitive
823 elements in eukaryotic genomes', *Mobile DNA*, 6(1). doi: 10.1186/s13100-015-0041-9.
- 824 Benson, G. (1999) 'Tandem repeats finder: A program to analyze DNA sequences', *Nucleic
825 Acids Research*, 27(2), pp. 573–580. doi: 10.1093/nar/27.2.573.
- 826 Bickhart, D. M. *et al.* (2017) 'Single-molecule sequencing and chromatin conformation
827 capture enable de novo reference assembly of the domestic goat genome', *Nature
828 Genetics*, 49(4), pp. 643-650. doi: 10.1038/ng.3802.
- 829 Bolger, A. M., Lohse, M. and Usadel, B. (2014) 'Trimmomatic: A flexible trimmer for Illumina
830 sequence data', *Bioinformatics*, 30(15), pp. 2114–2120. doi:
831 10.1093/bioinformatics/btu170.
- 832 Burge, C. and Karlin, S. (1997) 'Prediction of complete gene structures in human genomic
833 DNA', *Journal of Molecular Biology*, 268(1), pp. 78–94. doi: 10.1006/jmbi.1997.0951.
- 834 Camacho, C. *et al.* (2009) 'BLAST+: Architecture and applications', *BMC Bioinformatics*, 10:
835 421. doi: 10.1186/1471-2105-10-421.
- 836 Chin, C. S. *et al.* (2013) 'Nonhybrid, finished microbial genome assemblies from long-read
837 SMRT sequencing data', *Nature Methods*, 10(6), pp. 563–569. doi:
838 10.1038/nmeth.2474.
- 839 Down, T. A. and Hubbard, T. J. P. (2002) 'Computational detection and location of
840 transcription start sites in mammalian genomic DNA', *Genome Research*, 12(3), pp.
841 458–461. doi: 10.1101/gr.216102.
- 842 Eddy, S. R. (2002) 'A memory-efficient dynamic programming algorithm for optimal
843 alignment of a sequence to an RNA secondary structure', *BMC Bioinformatics*, 3: 18.
844 doi: 10.1186/1471-2105-3-18.
- 845 English, A. C. *et al.* (2012) 'Mind the Gap: Upgrading Genomes with Pacific Biosciences RS

846 Long-Read Sequencing Technology', *PLoS ONE*, 7(11): e47768. doi:
847 10.1371/journal.pone.0047768.

848 Goujon, M. *et al.* (2010) 'A new bioinformatics analysis tools framework at EMBL-EBI',
849 *Nucleic Acids Research*, 38(SUPPL. 2): W695-699. doi: 10.1093/nar/gkq313.

850 Grabherr, M. G. *et al.* (2011) 'Full-length transcriptome assembly from RNA-Seq data
851 without a reference genome', *Nature Biotechnology*, 29(7), pp. 644–652. doi:
852 10.1038/nbt.1883.

853 Griffiths-Jones, S. *et al.* (2003) 'Rfam: An RNA family database', *Nucleic Acids Research*,
854 pp. 439–441. doi: 10.1093/nar/gkg006.

855 Griffiths-Jones, S. *et al.* (2006) 'miRBase: microRNA sequences, targets and gene
856 nomenclature.', *Nucleic Acids Research*, 34(suppl_1), pp. D140–D144. doi:
857 10.1093/nar/gkj112.

858 Groenen, M. A. M. *et al.* (2012) 'Analyses of pig genomes provide insight into porcine
859 demography and evolution', *Nature*, 491(7424), pp. 393–398. doi:
860 10.1038/nature11622.

861 Hackl, T. *et al.* (2014) 'Proovread: Large-scale high-accuracy PacBio correction through
862 iterative short read consensus', *Bioinformatics*, 30(21), pp. 3004–3011. doi:
863 10.1093/bioinformatics/btu392.

864 Hubley, R. *et al.* (2016) 'The Dfam database of repetitive DNA families', *Nucleic Acids
865 Research*, 44(D1), pp. D81–D89. doi: 10.1093/nar/gkv1272.

866 Humphray, S. J. *et al.* (2007) 'A high utility integrated map of the pig genome.', *Genome
867 Biology*, 8(7), p. R139.

868 Koren, S. *et al.* (2017) 'Canu: Scalable and accurate long-read assembly via adaptive k-mer
869 weighting and repeat separation', *Genome Research*, 27(5), pp. 722–736. doi:
870 10.1101/gr.215087.116.

871 Koren, S. *et al.* (2018) 'De novo assembly of haplotype-resolved genomes with trio binning',
872 *Nature Biotechnology*, 36, pp. 1174-1182. doi: 10.1038/nbt.4277.

873 Kurtz, S. *et al.* (2004) 'Versatile and open software for comparing large genomes.', *Genome*

874 *Biology*, 5(2), p. R12. doi: 10.1186/gb-2004-5-2-r12.

875 Lefranc, M. P. *et al.* (2015) 'IMGT R, the international ImMunoGeneTics information system
876 R 25 years on', *Nucleic Acids Research*, 43(D1), pp. D413–D422. doi:
877 10.1093/nar/gku1056.

878 Lewis, S. E. *et al.* (2002) 'Apollo: a sequence annotation editor.', *Genome Biology*, 3(12), p.
879 RESEARCH0082. doi: 10.1186/gb-2002-3-12-research0082.

880 Li, H. and Durbin, R. (2009) 'Fast and accurate short read alignment with Burrows-Wheeler
881 transform', *Bioinformatics*, 25(14), pp. 1754-1760. doi: 10.1093/bioinformatics/btp324

882 Li, H. (2013). Aligning sequence reads, clone sequences and assembly contigs with BWA-
883 MEM. *ArXiv:1303.3997v1 [q-bio.GN]*.

884 Lowe, T. M. and Eddy, S. R. (1996) 'TRNAscan-SE: A program for improved detection of
885 transfer RNA genes in genomic sequence', *Nucleic Acids Research*, 25(5), pp. 955–
886 964. doi: 10.1093/nar/25.5.0955.

887 Meyers, S. N. *et al.* (2005) 'Piggy-BACing the human genome: II. A high-resolution,
888 physically anchored, comparative map of the porcine autosomes', *Genomics*, 86(6),
889 pp.739-752. doi: 10.1016/j.ygeno.2005.04.010.

890 Miller, J. R., Hindkjær, J. and Thomsen, P. D. (1993) 'A chromosomal basis for the
891 differential organization of a porcine centromere-specific repeat', *Cytogenetic and*
892 *Genome Research*, 62(1), pp. 37–41. doi: 10.1159/000133441.

893 Nattestad, M. and Schatz, M. C. (2016) 'Assemblytics: A web analytics tool for the detection
894 of variants from an assembly', *Bioinformatics*, 32(19), pp. 3021-3023. doi:
895 10.1093/bioinformatics/btw369.

896 Nguyen, D. T. *et al.* (2012) 'The complete swine olfactory subgenome: expansion of the
897 olfactory gene repertoire in the pig genome', *BMC Genomics*, 13(1), 584. doi:
898 10.1186/1471-2164-13-584.

899 Papatheodorou, I. *et al.* (2018) 'Expression Atlas: Gene and protein expression across
900 multiple studies and organisms', *Nucleic Acids Research*, 46(D1), pp. D246-D251. doi:
901 10.1093/nar/gkx1158.

902 Pendleton, M. *et al.* (2015) 'Assembly and diploid architecture of an individual human
903 genome via single-molecule technologies', *Nature Methods*, 12(8), pp. 780–786. doi:
904 10.1038/nmeth.3454.

905 Putnam, N. H. *et al.* (2016) 'Chromosome-scale shotgun assembly using an in vitro method
906 for long-range linkage', *Genome Research*, 26(3), pp. 342–350. doi:
907 10.1101/gr.193474.115.

908 Quinlan, A. R. and Hall, I. M. (2010) 'BEDTools: A flexible suite of utilities for comparing
909 genomic features', *Bioinformatics*, 26(6), pp. 841–842. doi:
910 10.1093/bioinformatics/btq033.

911 Ramos, A. M. *et al.* (2009) 'Design of a high density SNP genotyping assay in the pig using
912 SNPs identified and characterized by next generation sequencing technology', *PLoS*
913 *ONE*, 4(8), e6524. doi: 10.1371/journal.pone.0006524.

914 Robinson, J. T. *et al.* (2011) 'Integrative genomics viewer', *Nature Biotechnology*, 29(1), pp.
915 24–26. doi: 10.1038/nbt.1754.

916 Sayers, E. W. *et al.* (2010) 'Database resources of the National Center for Biotechnology
917 Information.', *Nucleic Acids Research*, 38(Database issue), pp. D5-16. doi:
918 10.1093/nar/gkp967.

919 Servin, B. *et al.* (2012) 'High-resolution autosomal radiation hybrid maps of the pig genome
920 and their contribution to the genome sequence assembly', *BMC Genomics*, 13(1), 585.
921 doi: 10.1186/1471-2164-13-585.

922 She, R. *et al.* (2011) 'genBlastG: Using BLAST searches to build homologous gene models',
923 *Bioinformatics*, 27(15), pp. 2141–2143. doi: 10.1093/bioinformatics/btr342.

924 Simão, F. A. *et al.* (2015) 'BUSCO: Assessing genome assembly and annotation
925 completeness with single-copy orthologs', *Bioinformatics*, 31(19), pp. 3210–3212. doi:
926 10.1093/bioinformatics/btv351.

927 Skinner, B. M. *et al.* (2016) 'The pig X and Y Chromosomes: structure, sequence, and
928 evolution', *Genome Research*, 26(1), pp. 130–139. doi: 10.1101/gr.188839.114.

929 Slater, G. S. C. and Birney, E. (2005) 'Automated generation of heuristics for biological

930 sequence comparison', *BMC Bioinformatics*, 6, 31. doi: 10.1186/1471-2105-6-31.

931 Smit, A., Hubley, R & Green, P. (2013-2015). *RepeatMasker Open-4.0*. [Online]. Available:
932 <http://www.repeatmasker.org> [Accessed 16/05/2016].

933 Smit, A.F.A. & Hubley, R. (2008-2015) *RepeatModeler Open-1.0*. 2008-2015
934 <http://www.repeatmasker.org>

935 Walker, B. J. *et al.* (2014) 'Pilon: An integrated tool for comprehensive microbial variant
936 detection and genome assembly improvement', *PLoS ONE*, 9(11), e112963. doi:
937 10.1371/journal.pone.0112963.

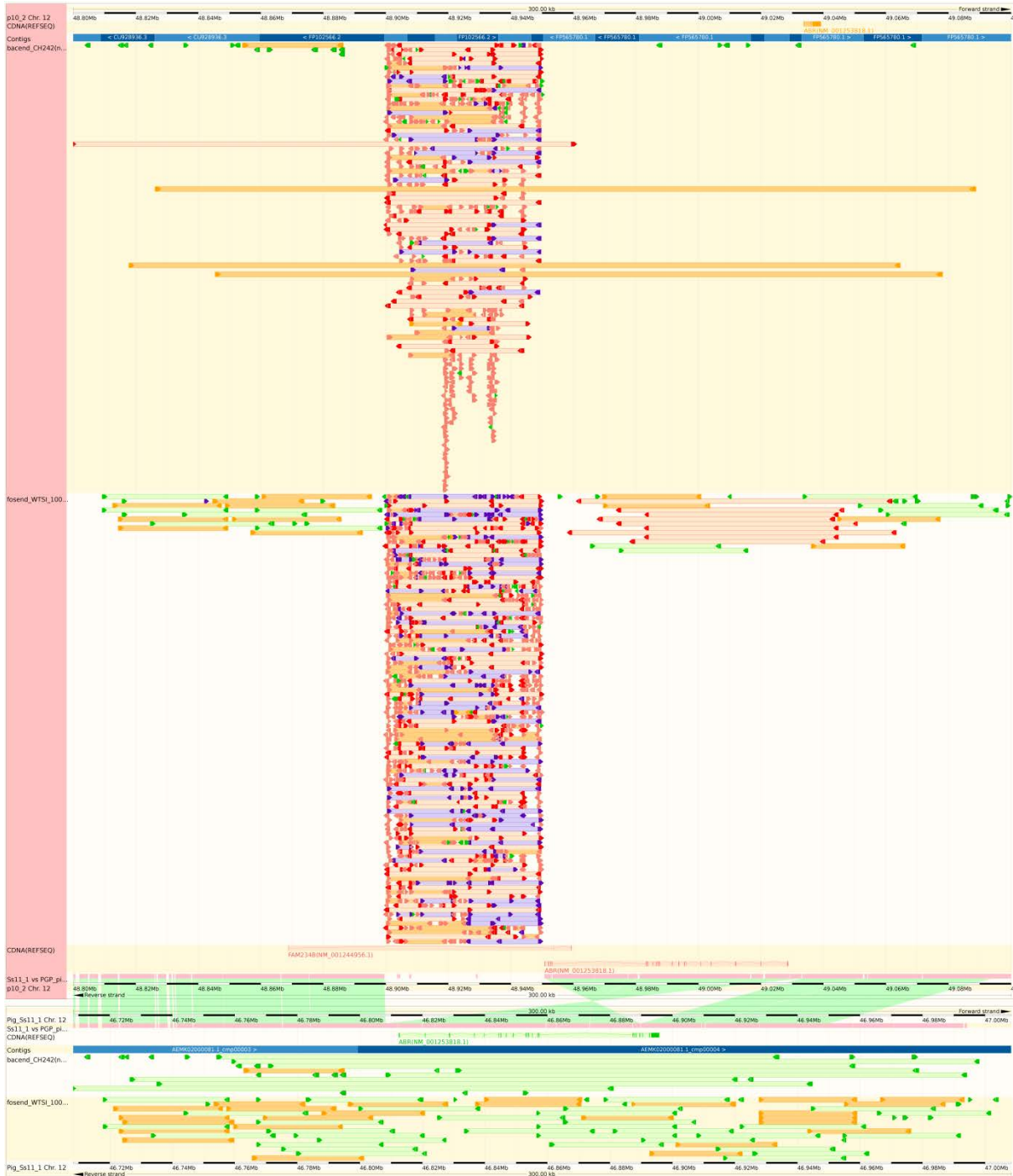
938 Warr, A. *et al.* (2015) 'Identification of Low-Confidence Regions in the Pig Reference
939 Genome (Sscrofa 10.2)', *Frontiers in Genetics*, 6, 338. doi: 10.3389/fgene.2015.00338.

940 Zhang, J. *et al.* (2014) 'PEAR: A fast and accurate Illumina Paired-End reAd mergeR',
941 *Bioinformatics*, 30(5), pp. 614–620. doi: 10.1093/bioinformatics/btt593.

942

943 **5. Further supplementary figures**

944 The following figures (Supplementary Figures SF12-16) illustrates improvements in the
945 assemblies as discussed in the main paper text.



946
947 **Supplementary Figure SF12:** Illustration of improvement in local order and orientation and
948 reduction in sequence redundancy
949 The alignment of isogenic CH242 BAC end and WTSI_1005 fosmid end sequences with the
950 SsCrofa10.2 (upper panel with pink bar on left hand side) and SsCrofa11.1 (lower panel).

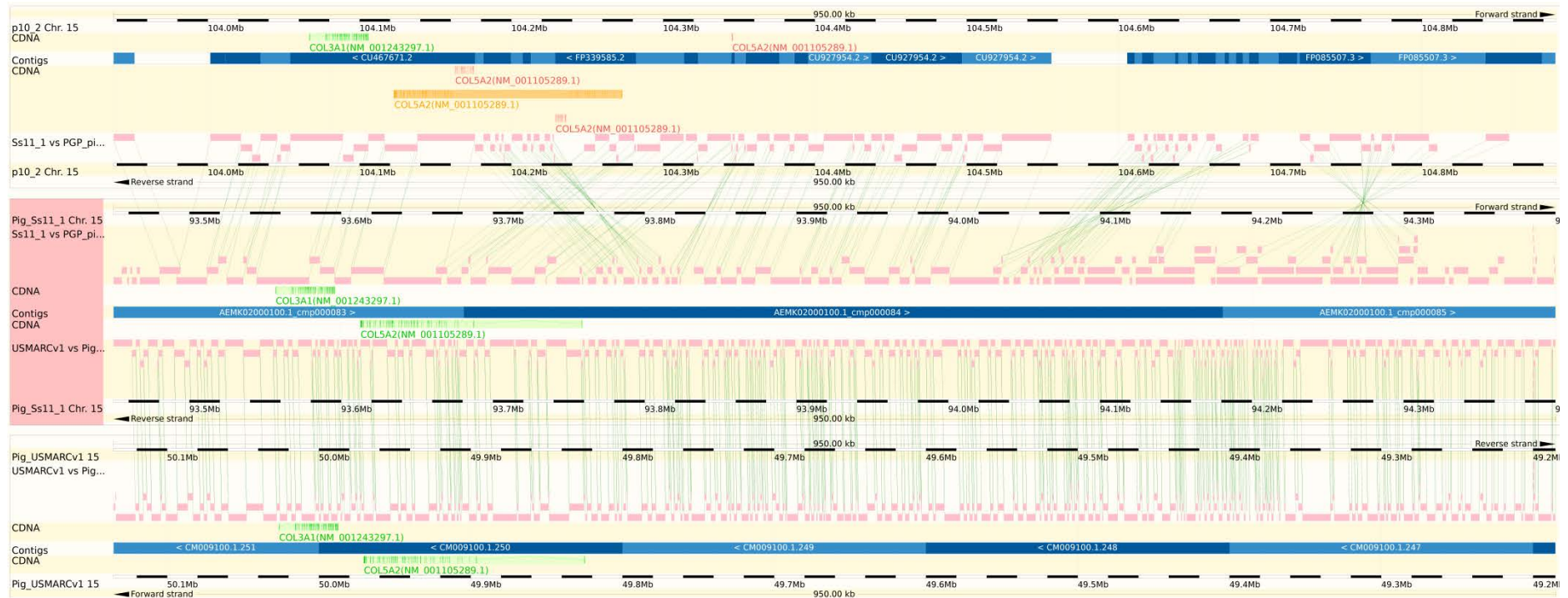
951 Red arrows indicate incorrect orientation of the paired end sequences, purple arrows are
952 sequences which are present multiple times, green and orange arrows indicate the end
953 sequences are correctly oriented. The distances between correctly oriented end sequences
954 are as expected (green) or either greater or less than expected (orange) for the clone insert
955 size for the fosmid or CH242 BAC libraries.

956

957

958 **Supplementary Figure SF13:** gEVAL comparison of Sscrofa10.2, Sscrofa11.1 and USMARCv1.0 at *COL3A1*, *COL5A2* loci.

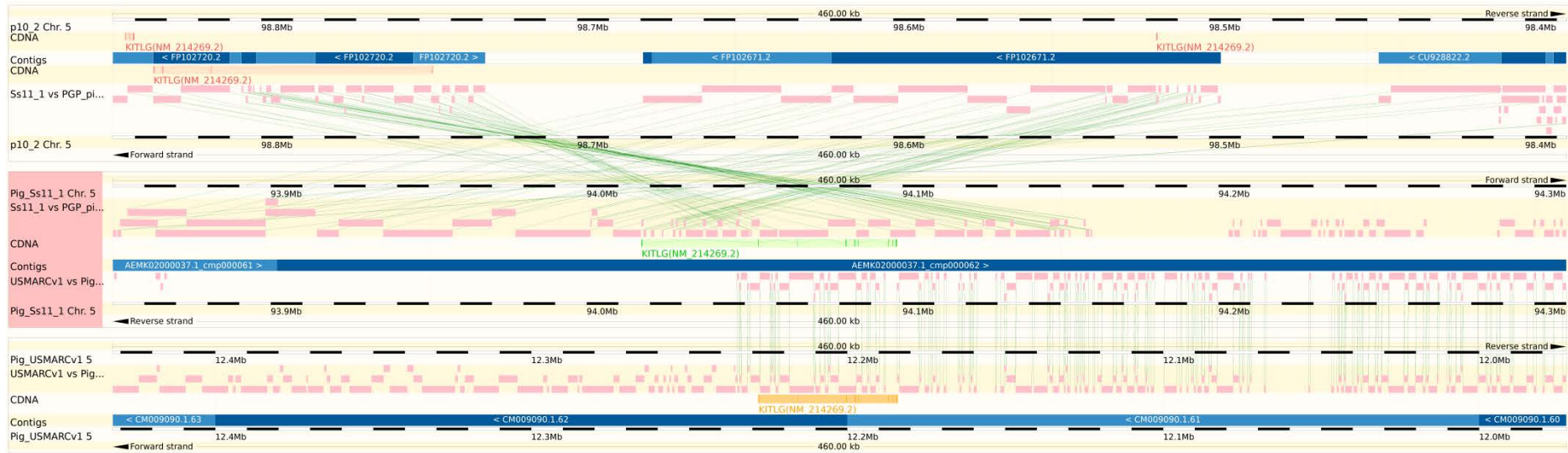
959



960

961 In the new assembly (Sscrofa11.1, middle row marked with pink vertical block) an improved gene model for *COL5A2* can be annotated; in the
962 previous assembly (Sscrofa10.2, upper row) the order and orientation of sequence contigs within BAC clone CH242-40P12 (ENA: FP339585.2)
963 are not resolved. There is good agreement between the Sscrofa11.1 (middle row) and the USMARCv1.0 (lower row) although the
964 USMARCv1.0 assembly of SSC15 is inverted relative to Sscrofa11.1.

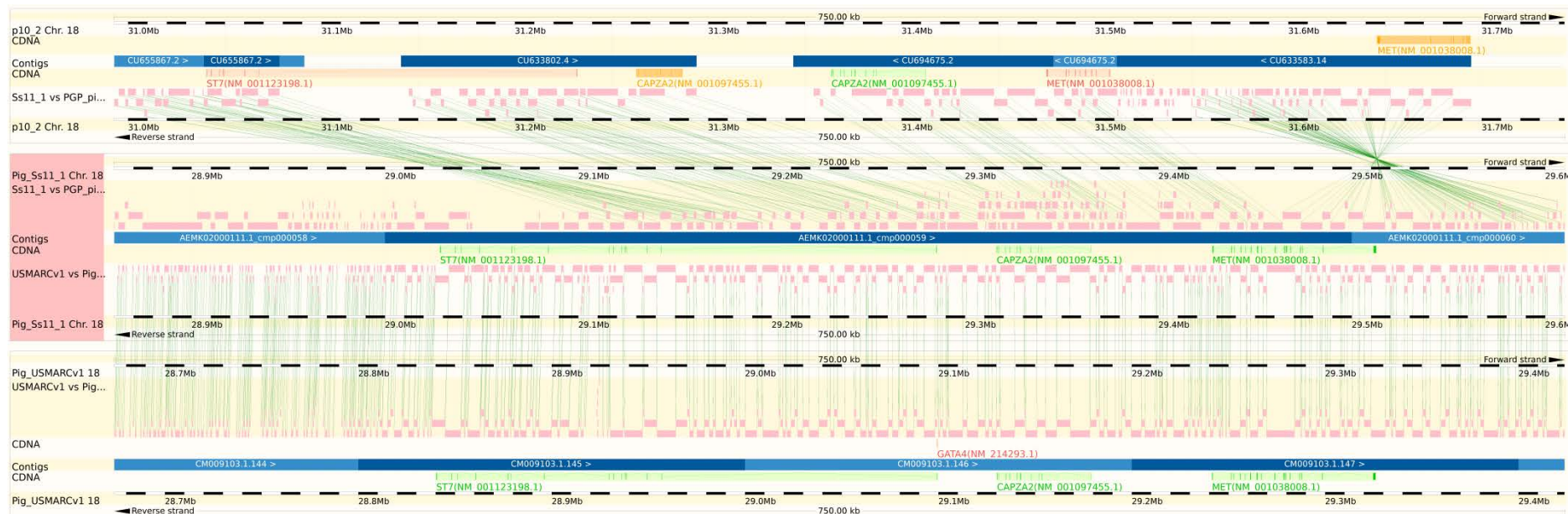
965 **Supplementary Figure SF14:** gEVAL comparison of Sscrofa10.2, Sscrofa11.1 and USMARCv1.0 at the *KITLG* locus.



966
 967 The new assembly (Sscrofa11.1, middle row with pink vertical block at left hand side) resolves the sequences encoding *KITLG* which were split
 968 across two small scaffolds in Sscrofa10.2 (upper row). Although there is good agreement between Sscrofa11.1 (middle row) and USMARCv1.0
 969 (lower row) assemblies in the right hand half of the region on SSC5 above, there is additional sequence present in the Sscrofa11.1 assembly
 970 between *DUSP6* and *KITLG*, the gene model for *KITLG* appears incomplete in the USMARCv1.0 assembly. Again the USMARCv1.0 is inverted
 971 relative to Sscrofa11.1.

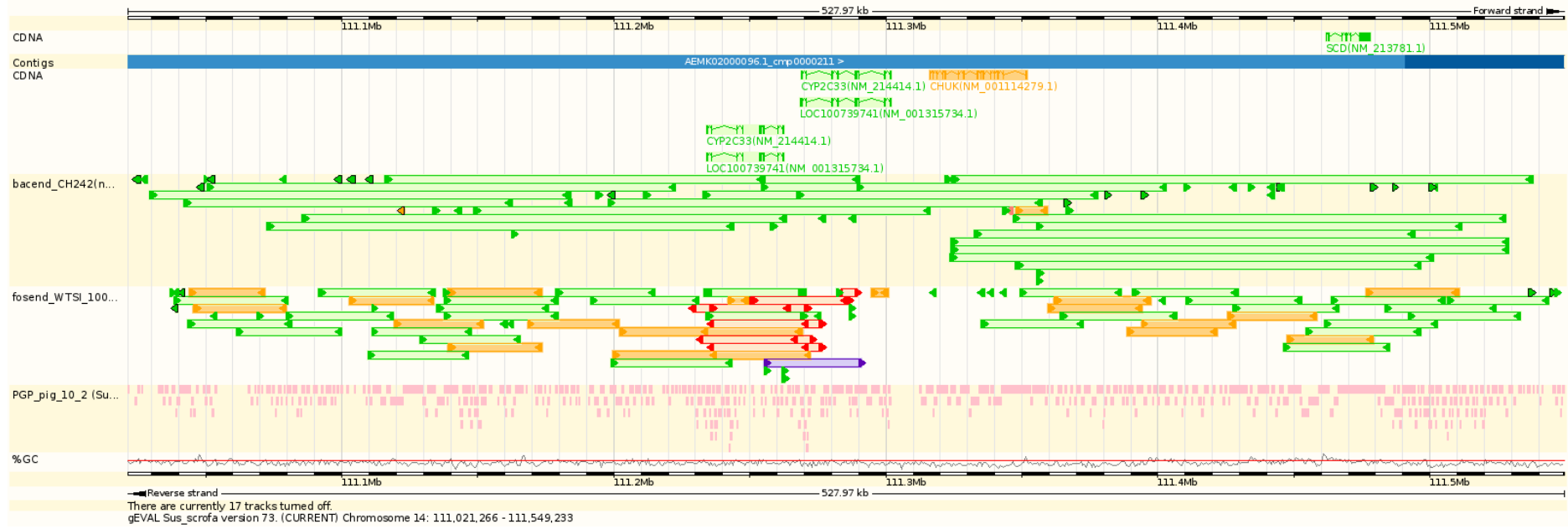
972

973 **Supplementary Figure SF15: gEVAL comparison of Sscrofa10.2, Sscrofa11.1 and USMARCv1.0 across the *ST7*, *CAPZA2* and *MET* loci on**
 974 **SSC18**



975
 976 The new assembly (Sscrofa11.1, middle row with pink block at left hand side) resolves the coding sequences for i) *ST7* that were previously
 977 split across two small scaffolds; *CAPZA2* that was similarly split across two small scaffolds; and iii) the *MET* sequences that were previously
 978 split as a result of an error in the orientation of the sequence drawn from BAC clone CH242-385N7 (ENA: CU633583.14) with respect to the
 979 sequence from BAC clone CH242-150K23 (ENA: CU694675.2) that harbours parts of the *MET* locus. This error in the incorporation of the
 980 CH242-385N7 (ENA: CU633583.14) in the Sscrofa10.2 assembly (upper row) is particularly unfortunate as this BAC had been sequenced to
 981 finish quality. There is good agreement between the Sscrofa11.1 (middle row) and USMARCv1.0 (lower row) assemblies with both SSC18
 982 assemblies also being in the same orientation.

983 **Supplementary Figure SF16: Absence of *ERLIN1* gene, duplication of *CYP2C33***



984

985